# Production- and Value Analysis of Hydraulic Fractured Wells in The Netherlands

Thomas Leo

Technische Universiteit Delft

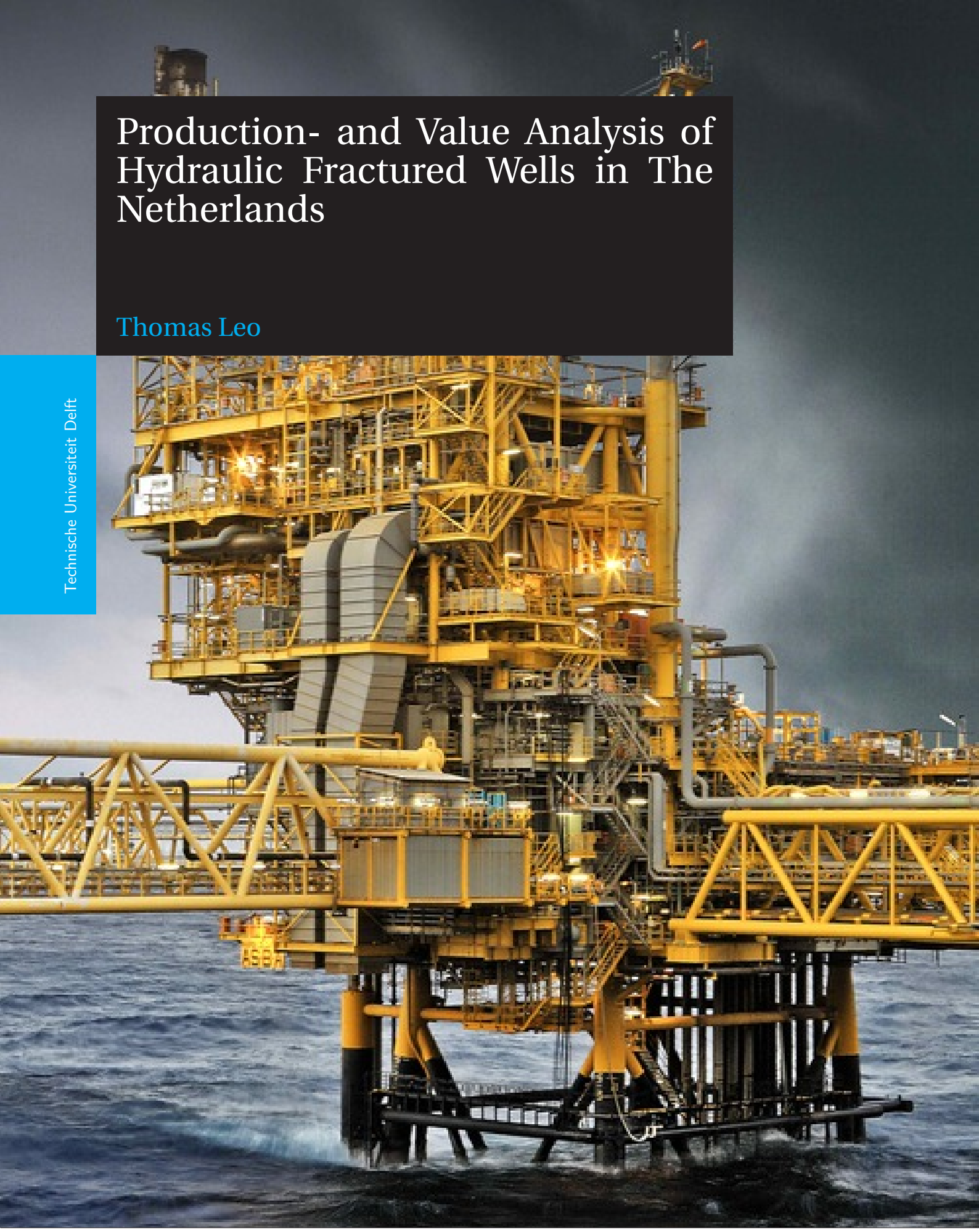

TU Delft Delft University of Technology

Challenge the future

# Production- and Value Analysis of Hydraulic Fractured Wells in The Netherlands

by

**Thomas Leo**

in partial fulfillment of the requirements for the degree of

**Master of Science**
in Applied Earth-sciences

at the Delft University of Technology,
to be defended publicly on Friday February 3, 2017 at 12:00 AM.


| | | |
|---|---|---|
| Student Number: | 4022505 | |
| Supervisors: | Prof. Dr. P.L.J. Zitha, | TU Delft |
| | Dr. Ir. R. R. G. G. Godderij | EBN B.V. |
| Thesis Committee: | Prof. Dr. P.L.J. Zitha | TU Delft |
| | Dr. A. Barnhoorn, | TU Delft |
| | Dr. H. Hajibeygi, | TU Delft |
| | Dr. Ir. R. R. G. G. Godderij, | EBN B.V. |
| | Ir. T. D. Huijskes | EBN B.V. |




TU Delft Delft University of Technology

# ABSTRACT

Hydraulic fracturing is a stimulation method to serve the enhancement of well productivity. The fracture creates a high conductive pathway into the formation. This improves the flow performance, bypasses damage and possibly connects additional dynamic gas. In the Netherlands, 252 wells were hydraulically fractured since 1954. This constitutes less than 10% of the amount of wells drilled in the same period. The objective of this project is to achieve more insights regarding the circumstances under which a hydraulic fracture is performed. The goal is to find a quantitative relationship that will lead to an improved performance for future fracturing campaigns.

To that end, hydraulic fracturing treatments executed on vertical gas wells have been investigated through analysis of their production behavior. A repeatable method consisting of five steps has been defined. Firstly, the critical flowrate is determined by Turner's equation. This method has been selected to avoid modeling of huff 'n puff production behavior. The second step is the use of the Decline Curve Analysis (DCA) to predict a range of ultimate production volumes. It should be noted that there is often an absence of stabilized production trends within the production data. As such, Rate Transient Analysis (RTA) has been used to perform the final three stages. These stages consists of material balances, history matches and forecasts. Moreover, an economic evaluation to quantify the commercial effects of hydraulic fracturing is performed. With hydraulic fracturing typically featuring a production acceleration, the increment in net present value (NPV) is a robust measure to define the success of a fracturing treatment.

In technical terms out of 38 investigated fractures, a total of 37 fractures had an increment in the productivity index (PI). An average increment factor of 2.8 has been determined after the well was fractured. Properties causing the highest increment in PI are low matrix permeability and a large fracture half length. The timing of the fracturing treatment has significant impact on the economic success. The earlier a fracture is set within a well's production life, the higher is the chance of economic success. Gas reservoirs depleted less than 35% of their initial pressure show the highest gains. By analyzing wells that are immediately fractured, it came to light that the connected dynamic GIIP has a major influence on a positive incremental NPV. Another important factor for economic success are the fracture properties. All fracturing treatments pumped with more than 100,000 kg of proppant did yield high production gains. In addition to these effects, a relationship between half length and quantity of pumped proppant has been established. Last but not least, in the recovery factors of wells that were immediately fractured, an interesting trend has been observed.

# ACKNOWLEDGEMENTS

This report is to fulfill the graduation requirements of the section Petroleum Engineering of The University of Technology Delft.

The graduation internship is performed within the technology department of EBN B.V. at Utrecht, The Netherlands. As a 100-percent state participation, EBN is responsible for a great deal of the income obtained by the Dutch State from gas and oil extraction from the Dutch subsurface. For the production of natural gas and oil, EBN cooperates closely with operators.

I would like to thank everyone who made this project possible. First of all EBN B.V. for offering me the place to execute my research, especially the technology department. A big thanks to my daily supervisors, Raymond Godderij and Thijs Huijskes, for their support and help during the months. Their expertise on production engineering, and especially hydraulic fracturing, were of great importance. It was a pleasure to work with them.

Further I would like to thank Delft University of Technology Department of Geoscience and Engineering and especially Prof. Dr. P.L.J. Zitha for providing support and guidance during the project.

The analysis within this project are performed within the software packages of IHS Harmony and Kappa. I am grateful to both companies for generously supporting this project with their software.

I am grateful to the operators for sharing their production data and technical reports.

Further I want to thank all other colleagues in the department, especially the trainees and interns for a great time.

Last but not least, I want to thank all my family, friends and girlfriend for their support during the months.

*Thomas Leo*
*Utrecht, January 2017*

# CONTENTS

# 1

# INTRODUCTION

Gas production in the Netherlands has been decreasing during the last couple of years. Since 2008 there is a decreasing production trend observable, while in the same period the associated production costs have almost doubled[1]. The bigger- and easily producible conventional gas reservoirs are getting mature. What remains are the smaller- and tougher producible fields, such as tight gas fields. Hydraulic fracturing could be the answer for efficient- and cost friendly way to produce these fields in The Netherlands.

In The Netherlands, 338 stimulation jobs by hydraulic fracturing are conducted since May 1954. The acid jobs were mostly executed in Zechstein reservoirs, while the propped hydraulic fractures were executed in tighter parts of the Rijnland, Rotliegend and Bunter&Limburg formations. Moreover, hydraulic fracturing could also be applied in conventional reservoirs to accelerate production. Clearly, hydraulic fracturing is quite common in The Netherlands, although it could be applied on a much larger scale[1]. Understanding in which cases economic value can be added by means of hydraulic fracturing can be very useful for future fracturing campaigns.

Therefore a production analysis on fractured wells on the Dutch continental shelf is performed by Rate Transient Analysis (RTA). RTA can be applied to analyze fractured wells that are in the pseudo steady state flow regime. In this regime, which comes after transient flow in early times of production, the reservoir is producing in boundary dominated flow. With RTA techniques, the reservoir and fracture properties can be modeled by material balances, history matches and forecasts. Since there is often an absence of stabilized production trends within the production rates, Decline Curve Analysis (DCA) is not applicable to a significant number of wells. The advantage of RTA is the prediction of more reliable forecasts as the analysis applies continuous production and flow pressure data to characterize the reservoir. There has already been performed research projects on RTA (Joo et al., 2015; Santacruz et al., 2015; Maxwell et al., 2013; Wie et al., 2014; Duong et al., 2011; Murminacho et al., 2015; Clarckson et al., 2010). However, these analysis were not conducted on vertical gas wells with single fractures, which is the case for a majority of fractured wells in The Netherlands. From a previous research project conducted by EBN on hydraulic fractured wells in The Netherlands, it came upon light that big frac jobs (>100,000 kg proppant) and proppants with the biggest diameters gave the best result on production increment[2]. This conclusion was based on analyzing technical end of frac reports made by operators on 95 fracturing treatments.

In this thesis-report 38 hydraulic fractures on the total of 338 were investigated for several reasons. First of all, the wells before 1994 are not taken under consideration. There is no sufficient information about the fracturing treatments and the daily production data is not properly stored within this period of time. Secondly, EBN is not partner in every well in The Netherlands. A good example are the wells in the Coevorden field, of which fifteen of them have been subjected to hydraulic fracturing. Also wells with incomplete or wrong pressure- and flowrate data are not taken into account, since this results in improper outcomes. An example of wrong pressure data are pressure measurements done after the choke. With these pressures it is not possible to get a reliable history match, since the pressure are not representing the actual flowing tubing head pressures. Thirdly, no oil fields have been examined in this report. More or less 30% of the hydraulic fractured wells were oil producing. Fourthly, the horizontal wells are not taken into account. The horizontal wells are modeled in IHS Harmony by RTA, but the results cannot be compared to vertical wells. It is difficult to value a single fracture in a multi-fractured horizontal well. It is unlikely that every single frac in a multiple fractured horizontal well has the same gain in terms of production. Lastly, the total numbers of hydraulic

fractured wells also includes exploration wells. From these exploration wells there is no production data available to perform a rate transient analysis.

## 1.1. RESEARCH OBJECTIVES

The main objective of this study is to asses the impact of a hydraulic fracture on the production behavior of a gas well. To fulfill the main objective of this study, several goals have been set:

- To understand the mechanisms involved in hydraulic fracturing
- To perform a proper technical analysis by Rate Transient Analysis
- To determine the added value of a hydraulic fracture campaign in terms of economics
- To find a quantitative relationship between the circumstances under which a fracture is set and its associated success

Increased knowledge regarding the circumstances under which a hydraulic fracture is performed and the actual success on the quality of the fracture can be very useful for future fracturing campaigns. One can think about the circumstances as in reservoir parameters as well as the operational aspects. The reservoir behavior is analyzed with rate transient analysis, while the operational aspects are derived from technical reports about the fracturing treatments filled by the operators.

## 1.2. RESEARCH OUTLINE

The principle of hydraulic fracturing is explained in Chapter 2. This chapter will briefly describe the history of fraccing, the mechanisms involved and the actual risks. In Chapter 3 the methodology of this research is described. The workflow to perform a technical analysis on the production data is first explained, while the other sections go further into detail about the determination of the liquid loading rate and the use of Rate Transient Analysis in IHS Harmony. The analytical models describing the wells and reservoirs are separately explained Chapter 4. This includes decline curve analysis, material balance analysis, performing a history match and finally creating a forecast. The results are given in Chapter 5, and are subdivided in wells with and without pre-frac data. Also some exceptions are taken into account, including wells that have been subjected to hydraulic fracturing stimulation but the operations failed. The discussion is given in Chapter 6 and goes further into detail of assumptions and uncertainties. Finally, the conclusions based on the results are given in Chapter 7. In Chapter 8 recommendations are given for future studies.

# 2

# HYDRAULIC FRACTURING

Hydraulic fracturing was introduced in the late 1940's as a commercial stimulation tool. In 1947 it was presented to the petroleum industry by executing the first treatments on the Klepper 1 well in the Hugoton field in the USA by Stanolind[3]. Even though the unsuccessful outcome of the tests, Halliburton Oil Well Cementing Company patented the process. In 1949 it was commercially accepted by the industry, after it had increased the production of two wells enormously. The first was in Stephens County, Oklahoma, and cost only 900 USD. The second one was executed in Archer County, Texas, and came with a price of 1000 USD[4]. During this time period, the frac was more or less a complete gamble. It was a hit-or-miss proposition, since there was little data available resulting in little knowledge. However, the successive 12 months after the 2 successful performed treatments, 332 wells had been hydraulic fractured, with an total increment in production of 75%. Throughout the 1960's and 1970's the data quality improved due to research and better models could be generated to control the fracture job. Nowadays, more cost effective and efficient treatments could be done for enhancing well productivity[5][6]. Since the breakthrough, millions of fractures have been pumped (The Society of Petroleum Engineers estimates 2.5 million fracs worldwide) over the past 60 years[7]. Especially the combination of horizontal wells with hydraulic multi-fracs to produce the shale-gas reservoirs in the USA are enormously popular. It is not unusual to put up to 40 frac stages in a well nowadays. It is estimated that at least 30% of the recoverable oil and 90% of the gas reserves in the USA can be attributed to the application of hydraulic fracturing.

Hydraulic fracturing stimulation was introduced in the Netherlands in the mid 1950's. Since 1954 till September 2015, 252 wells have been hydraulic fractured, both on- and offshore, according to the SodM-report from February 2016[8]. This involves a total of 338 fractures within the Netherlands as can be observed in table 2.1.

Table 2.1: Numbers of hydraulic fractured wells in the Netherlands until September 2015

| | **Number of Fractured Wells** | **Number of Fracs** |
|---|---|---|
| **Onshore** | *155* | *219* |
| **Offshore** | *97* | *119* |
| **Total** | *252* | *338* |

The 252 wells that are hydraulic fractured in The Netherlands are given in figure 2.1. In this figure the number of treatments per year can be seen. There is no successive trend observable in the amount of hydraulic fracturing treatments. It seems fracturing campaigns are coming in periods. In the period between 1960 and 1966, the first considerable amount of wells have been fractured. The most active period proceeds from 1979 till 1992: almost the half of all treatments are performed within these 13 years. Within this period, the highest amount of fracturing treatments per year is conducted: 16 wells were treated in 1986. Nowadays, the average amount of treated wells is more or less five per year.

Hydraulic fracturing has been, and will remain, one of the primary engineering tools for improving production. Hydraulic fracturing is placing a highly conductive channel deep into the reservoir, which creates three different effects: improvement of the flow performance, bypass of damage and an opportunity to connect extra recoverable gas.

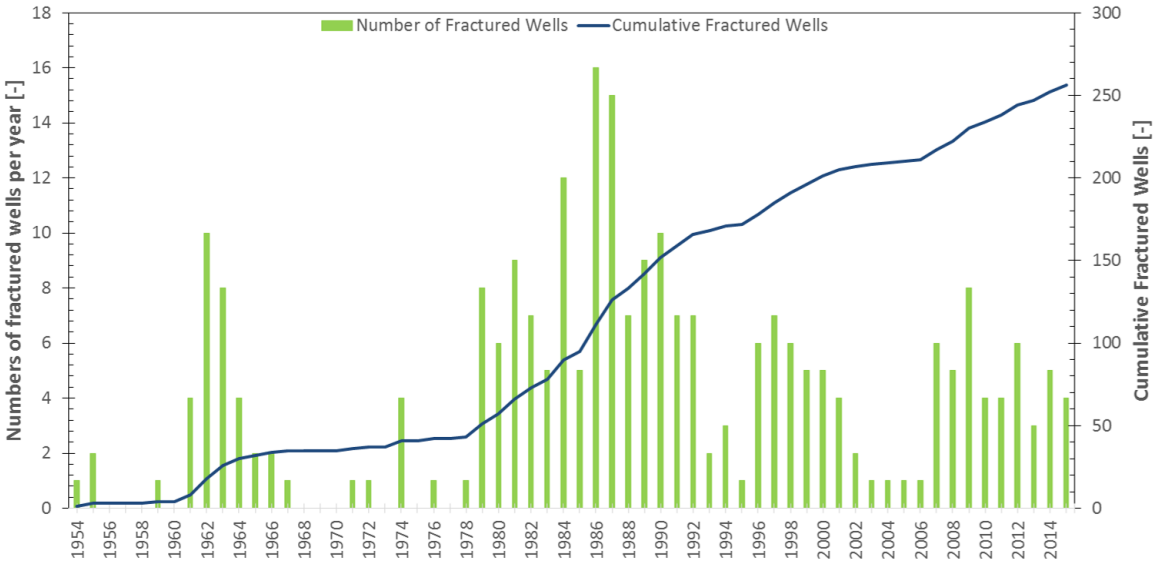


Figure 2.1: Overview of the number of fractured wells from 1954 till 2015 in The Netherlands. The green bars indicate the number of fractured wells per year, while the blue line expresses the cumulative amount of fractured wells[1].

The principle of hydraulic fracturing is the enhancement of the well productivity. Gas is located within the pore-spaces of the reservoir-rock in the subsurface. When the permeability of the rock is between 0.5 and 20 mD, the reservoir is called conventional. The hydrocarbons flow easily to the production well and there is no stimulation needed to get sufficient recoveries. However, some hydrocarbons are trapped within formations with permeability lower than 0.5 mD. These unconventional reservoirs include the tight gas fields, coal bed methane and shale gas. The unconventional reservoirs are the main targets for hydraulic fracturing. The frac enhances the properties of the reservoir rock such that the hydrocarbons can be extracted economically. Tight gas reservoirs are normally fracced with a single frac, while shale gas reservoirs are produced with multifrac horizontal wells, due to their very low permeability (<100 nD). However, this report will focus on the tight gas fields and the conventional reservoirs that have been produced for longer time. All wells that are used within this project are vertical.

The stimulation technique creates cracks in the reservoir rock by injecting fluids under very high pressure. The fluids are injected in the wellbore at a rate high enough to increase pressure downhole to exceed the strength of the rock. This leads to the frac in the reservoir rock, normally a vertical plane which grows in two opposite directions. The fracture changes the inflow performance due to change in pressure drop near the wellbore. This ensures the radial flow changes to linear flow. Furthermore, the fracture provides a high conductive path from formation into the wellbore. It allows the hydrocarbon to bypass the damaged zone around the wellbore caused by cementation of the liner or fluid used during drilling, resulting in higher production rates. Also trapped hydrocarbons within the formation could be made mobile, resulting in an increase of recoverable gas reserves. This chapter will describe all operational aspects involved within the hydraulic fracturing technique. Furthermore, the mechanisms behind the stimulation and risks are discussed.

## 2.1. OPERATIONAL ASPECTS

The operations always start with a mini frac or a breakdown test before the main stimulation is performed. The mini frac test is regarded in the industry as the most reliable method to determine essential formation properties and to assess wellbore condition. The test is an injection falloff diagnostic test performed without proppant and the intent is to break down the formation to create a short fracture during the injection period. The pressure data gathered during the test could give valuable information about fracture closure pressure, fluid leak off coefficients and reservoir pressure. Based on this information, the pump schedule for the main hydraulic fracture stage will be developed [9].

There are normally four stages involved by the execution of the main hydraulic fracture. These consists of the pre-pad, pad, slurry and flushing stage.

1. Pre-pad stage. This stage is executed with a dilute acid such as hydrochloric or muriatic acid. This will

dissolve cement debris in the wellbore and provides a free path for the later injected fluids to flow easily into the reservoir. The pre-pad stage develops a relatively large radius of curvature near the wellbore. This reduces the pressures losses during the mean treatment.

2. Pad stage. The pad stage fills the wellbore with clean fluid (without proppant) and initiates the fracture. It must create sufficient fracture width to allow space for placement of proppant material in the next stage.

3. Slurry stage. This stage consists normally of several subsections of pumping frac fluid combined with the desired proppant. The successive pumping stages have increasing proppant concentration to enhance the same proppant density within the fracture. The first pumping stage will finally reach the tip, created by the pad-stage. Normally the concentration of this first stage consists of approximately 1 PPG (Pounds Proppant per fluid Gallon) when injected. However, the concentration of the first stage has increased several times due to the leak-off of the the carrying fluid into the formation. The leak-off of the carrying fluid depends highly on the permeability of the formation. The higher the permeability within the reservoir, the higher the leak-off rate. Finally the first stage has concentrated to a 8 PPG stage at the end of a fracturing treatment, when it has reached the tip. The successive pumping stages will all have increasing concentrations of proppant. Since the stages have to cover less distance through the fracture, there will be less leak-off of carrying fluid and the concentration will be less influenced. Finally the last injection stage will have a concentration of 8 PPG, leading to a uniform density of proppant. The proppant schedule for a normal executed job can be observed in figure 2.2. The green dashed line indicates the proppant concentration as function of the slurry volume with a normal procedure [10].

   Besides the normal procedure, it is also possible to execute a Tip Screen Out fracturing procedure (TSO), also known as a fracpack. This has a different pumping schedule compared to the procedure described above. The proppant schedule for a TSO job can also be observed in figure 2.2 by the blue dashed line. As can be seen in the figure it actually consists of two stages. The first is the early stage which is compared with the normal procedure quite long and the proppant concentration quite low. These early stages are intended to migrate to the fracture boundary and stop fracture propagation at the desired time. With propagation halted, fracture width will continue to increase and additional proppant will begin to pack back from the tip. This first stage is called the pin stage, as it is shaping the geometry of the fracture in place. As pressures indicate that the tip screen out is formed, the pumping pressure at the surface will be increased. This forces as much proppant as possible into the fracture, which ensures creation of extra width and proppant loading at the wellbore, resulting in higher flow capacity. TSO procedures are normally conducted in reservoirs with higher permeabilities [11] [12].

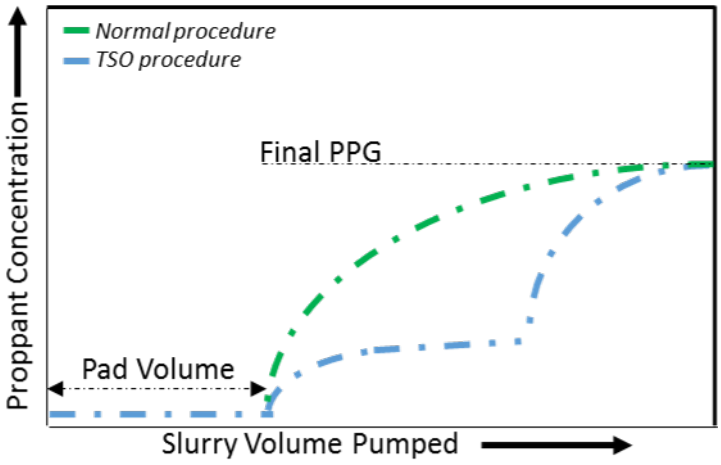


Figure 2.2: Proppant schedule for a normal job (indicated by the green dotted line) and a TSO executed job (indicated by the blue dotted line). Goal is in both procedures uniform concentration of proppant in the fracture.

4. Flushing stage. Injection of fresh water within the fracture to flush the excess proppant from the wellbore

After the stimulation process, the well requires a specific post-stimulation flow period to ensure proper preparation for long term production. This specific post-stimulation flow is also called the clean-up of the well: it is necessary to flow back the proppant and injection fluid located in the wellbore. Otherwise the remainings can reduce future performance or even kill the well if it forms a barrier around the wellbore. On the other hand, water that is not produced back could also assist production in a positive way. Recent work showed that minerals adsorb the water and become larger. These water-altered minerals could act as a proppant in small open fractures within the formation[7]. It is therefore, crucial that the clean-up procedure is conducted in the right way. Excessive flowback rates are known to cause proppant flowback or even fracture collapse [13].

All wells investigated in this report are analyzed by the operator after the treatment was executed. Post frac analysis can be done in commercial software packages as FracPro and needs pressure-, stress- and flowrate data gathered during the treatment. The post-frac analysis also results in the half length of the fracture, which is used in this project as input parameter for history matching during rate transient analysis.

## 2.2. FRACTURING FLUIDS

The fracturing fluids have made a major change over the past years. Operators started their first experimental treatments with a fracturing fluid composed of gasoline gelled with palm oil and crosslinked with naphthenic acid. The hazards and the associated high costs were the trigger to develop other fluids. Nowadays, four different classes of fracturing fluid are known: water-, foam-, oil- and acid based. In The Netherlands only water- and acid based treatments are executed. The vast majority of fracturing fluids use water as the base component with a proppant additive[14]. Almost 75% of the wells in The Netherlands is fractured with the proppant based fluid, while 25% is done via an acid treatment. The real numbers can be found in table 2.2.

Table 2.2: The distribution of fractured wells by fraccing fluids[8]

| | **Number of Proppant Fracs** | **Number of Acid Fracs** |
|---|---|---|
| **Onshore** | *165* | *54* |
| **Offshore** | *93* | *26* |
| **Total** | *258* | *80* |

### 2.2.1. ACID BASED FLUIDS

The acid based fluid is the oldest but not the most used method. The acid is used to etch channels in the reservoir rock by a chemical reaction. Therefore the acid should be able to dissolve in the rock, which is the case for reservoirs containing limestone, dolomite or calcite. The acids used are hydrochloric acids (HCl) or hydrofluoric acid (HF). The hydrochlorics acid are useful in these carbonate reservoirs, while the hydrofluoric acid dissolves quartz, sand and clay from the reservoir rocks[15]. Composition of the fluid depends on the type of rock and varies for almost every case. A huge advantage of fracturing by acids, is that there are no proppants needed to keep the fracture open.

### 2.2.2. PROPPANT CARRYING FLUIDS

Although the hydraulic fracture creates a highly conductive path during pumping, once pumping stops and the injected fluids leak off, the fracture will close and its desired effect vanished. To prevent this, the proppant is used. When the pumping stops and fluid flows back from the well, the proppant remains in place to keep the fracture open to create a conductive flow path. A standard composition is not common for the proppant carrying fluids. The fluids are developed to meet the specific needs of each reservoir. It will vary based on the site-specific depth, thickness and other characteristics of the target formation and proppant carrying capacities. Service companies that provide the additives have developed a number of compounds with similar functional properties to be used for the same purpose in different well environments. However, to give an global overview of the additives, the composition of a frac fluid compiled from data collected at the Fayetteville Shale Fracture Stimulation is given in figure 2.3.

The fluid consists for more than 90% of fresh water. The volume of proppant is the highest- and most important addition to the fluid. It covers almost 9% of the total volume. Usually the proppant particles are carried by the frac fluid into the fracture to keep the fracture open. The first propped fracture treatments were executed with sand dredged from riverbeds. Nowadays, the major proppants used includes ISO quality sand, resin coated-sand, ceramics and sintered bauxite[4]. The size of the proppant is very important for the

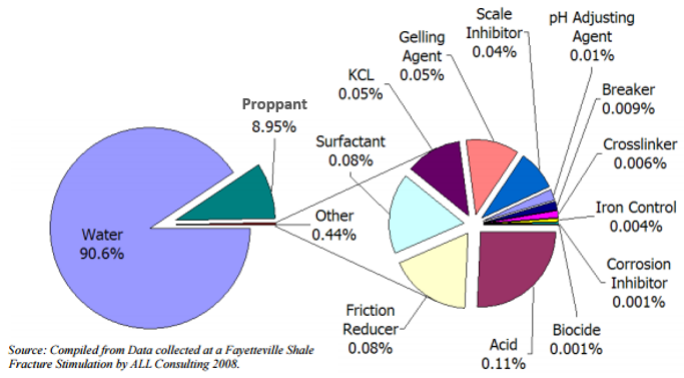


Figure 2.3: Composition proppant based fraccing fluid [16]

quality of the fracture, since it provides the desired conductivity. The sizes of proppants are measured in U.S. mesh sizes, and are always expressed in pairs who are representing the limits of grain sizes. The first number is the greatest grain size, while the second is the smallest. The first developed proppants were coming from the Ottowa mines in United States. The grains produced were all having grain sizes falling 20 and 40 mesh sizes. Since then, this became the standard and was called the 20/40 proppant. The sizes, with the converted IS-units, are summarized in figure B.1 in Appendix B.

The mostly used sizes in The Netherlands are the 12/18, 16/20, 16/30 and 20/40 mesh sizes. Also combinations of both can be used. Normally the larger mesh proppants will result in higher permeability than small mesh proppants. Since the stacking pattern of larger diameter-particles causes an higher permeability within the fracture. However the larger mesh proppants are more sensitive for mechanically failure, as they are easier to crush.

The other additives in the frac fluid are summarized in table 2.3 with their associated functions. This is only 0.44% of the fracture fluid and are mainly added to avoid negative side effects.

Table 2.3: Additives in the fraccing fluid

| **Name** | **Volume** | **Function** |
|---|---|---|
| Friction Reducer | *0.08%* | *Reduces friction pressure of fluid flowing through the pipe* |
| Surfactant | *0.08%* | *Modify surface or interfacial tension and prevent emulsions* |
| Acid | *0.11%* | *Reduction of fracture initiation pressure* |
| Gelling Agent | *0.05%* | *Initiate the frac and gelled water to carry some of the proppant* |
| Scale Inhibitors | *0.04%* | *Prevent mineral precipitates and eliminating blocking of tubing/equipment* |

## 2.3. MECHANISMS

As mentioned earlier, hydraulic fracturing increases the productivity of a reservoir which is achieved by three crucial principles which are explained in more detail in this section. The three principles are changing flow performance, bypassing of damage and possibly connecting extra recoverable gas to the well.

### 2.3.1. FLOW PERFORMANCE

The gas is flowing from the reservoir into the wellbore and is normally described with Darcy's law, which is simplified given in equation (2.1).

$$\frac{Q}{A} = \frac{k}{\mu}\frac{\Delta P}{\Delta x} \tag{2.1}$$

Where $Q$ stands for flowrate, $A$ for formation flow area, $k$ the matrix permeability, $\mu$ the viscosity of the liquid and $\Delta P/\Delta x$ is the pressure drop. Reservoir exploitation revolves around manipulating this equation. For example, artificial lift is used to increase the pressure difference between wellbore and reservoir, steam injection for lowering the viscosity of the liquid and water injection to maintain the reservoir pressure.

A wellbore of a vertical unfractured well produces normally with radial flow. Formations that have very low matrix permeabilities (which are the target formations for hydraulic fracturing), have also low flowrates

according to equation(2.1). Radial flow can be observed in figure 2.4. This is the topview of the reservoir and the green circle indicates the wellbore, while the red arrows are presenting the gas flow to the wellbore. When

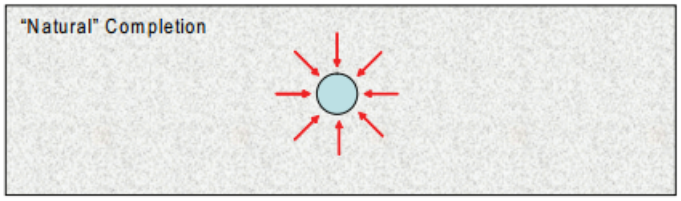


Figure 2.4: Topview of radial flow occurring in a unfractured well

a vertical well is hydraulically fractured, the flow pattern will change. The fracture will behave as a highly conductive path for the fluid and ensures the formation area ($A$) will increase. According to equation(2.1) this results in higher flowrates. The fluid will mostly enter perpendicular to the fracture, resulting in linear flow near the fracture. Further away from the fracture, the flow will become elliptical which will slowly change to radial flow again. The flow patterns are depicted in figure 2.5. This is again the topview of the reservoir where the circle is the wellbore, and the red arrows indicates the gas flow. The two critical parameters that a fracture

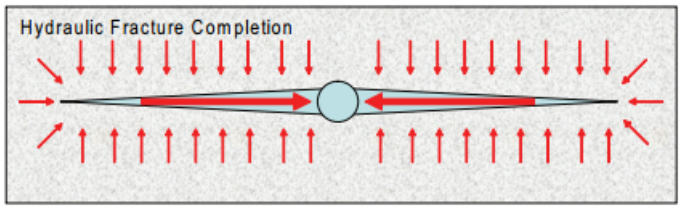


Figure 2.5: Topview of linear flow occurring in a fractured well

must possess to be successful are a long fracture half length and a high fracture conductivity. Since IHS Harmony is not capable of programming a finite conductive fracture, there is always an infinite conductive fracture assumed. Therefore, only linear flow occurs instead of bi-linear. With the bi-linear flow, there are actually two types of linear flow occurring. First there is the flow from the matrix to the fracture and second from the fracture to the wellbore. However in this study the permeability of the fracture is modeled so high that the pressure throughout the fracture is constant and there is only flow from the matrix to the fracture. A long half length represents thus a qualitative good fracture in the model.

### 2.3.2. BYPASS DAMAGE

Wellbore damage can reduce the productivity of a well tremendously. Damage can be caused by many reasons, both by drilling activities as well as natural reservoir processes. Drilling activities include for example the drilling fluids that are left behind during clean-up, and could be incompatible with the rocks. But also cementation processes can reduce productivity: cement debris can form a barrier around the wellbore. Natural reservoir processes as sand production or salt precipitation could also cause damage to the wellbore. Whatever the reason is, it is not influencing the inflow performance in a positive way. Normally the wells are treated with acid stimulation fluids or re-perforated to create flow paths through the damage barrier. However, sometimes the barrier is too hard to handle and hydraulic fracturing is the only solution. In figure 2.6 and 2.7 two situations are drawn. Figure 2.6 is representing the wellbore with damage before fracturing. The fracture bypasses the damaged layer, enhancing well productivity.

### 2.3.3. EXTRA RECOVERABLE GAS

Extra recoverable gas is the last possible added value of a hydraulic fracture. It is sometimes possible to connect extra dynamic gas to the well by creating a fracture. This happens when gas is locked in (possibly thin) unconnected and unperforated layers. This is shown in figures 2.8 and 2.9.

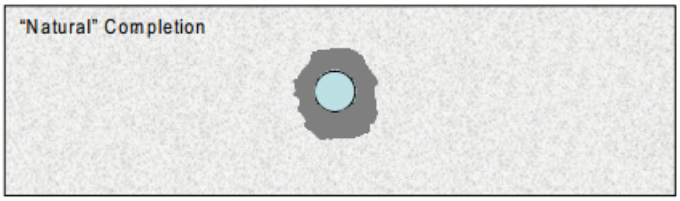


Figure 2.6: Damage around a non-fractured well. The productivity of the well is reduced by the damage.

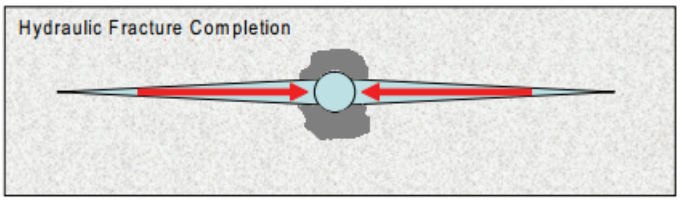


Figure 2.7: Damage bypass of a fractured well

## 2.4. RISK AND SAFETY

Although there are 252 wells hydraulically fractured in the Netherlands, this is only a small percentage of the amount of wells drilled. Still, there is a lot of skepticism going on about the risks and safety of fraccing. Two of the main discussion points are documented by the Fraser Institute [17] and includes:

1. Risk to surface- and ground water. Hydraulic fracturing could have a big effect on the quality of the surface and ground water for several reasons. First of all, the chemicals injected into the reservoir could be capable of migrating into the water-bearing zone and pollute drinking water. Secondly, the treatment consumes a considerable amount of fresh water and thirdly it produces a considerable amount of waste water. The US Environmental Protection Agency (EPA) conducted a research to the water pollution by hydraulic fracturing in 2015[18]. They concluded that there was no evidence that hydraulic fracturing treatments have led to widespread systematic impact on drinking water resources in the USA. Another research project by Jackson et al (2014), came up with the same conclusion[19]. The occurrence of migration of chemicals from the reservoir to the water bearing zone seems to be unlikely. They concluded on micro-seismic data that a fracture will not propagate more than 600 meter and almost all reservoirs are located deeper than 1000 meter. Since the fresh water-bearing zones are located not deeper than 300 meter, the fracture will not come in contact with this zone. In the USA a major part of the wells is hydraulically stimulated to produce from the shale-gas fields. These reservoirs are located shallower than the reservoirs in the Netherlands. Provided with this evidence it is even more unlikely that migration will appear in the Netherlands. A simpler pathway for groundwater pollution is through well integrity. If the casing or liner does not completely seal off the subsurface, the chemicals could leak off to the fresh water-bearing zones. Especially, the enormous pressures a well is subjected to during a treatment is a potential risk. If the cementation job is not properly conducted, cracks could form during a treatment and leakage or even collision could occur. Therefore, it is absolutely necessary the casing and liner are exposed to a pressure- and integrity test before a fracturing treatment is performed. However, the contamination incidents in America are still low, ranging from 0.1% in Ohio to 0.02% in Texas. The considerable amount of fresh water used during the treatments could be produced back for a certain part. However, there will always remain injected water in the reservoir. Compared to the water use in for example the agriculture, it is negligible. Besides, there are nowadays very efficient recycling processes, which are approaching a 90% recovery rate of fresh water.

2. Induced seismicity. Hydraulic fracturing could result in induced seismicity, better known as earthquakes. There are some good examples of hydraulic fracturing that has caused fault or fracture reactivation. Davies et al conducted a research on 198 hydraulically fractured wells and came up with the conclusion that hydraulic treatments usually generates very small magnitude earthquakes compared to other production processes. Processes such as reservoir impoundment, conventional oil- and gas field depletion, water injection for geothermal energy recovery and waste water injections are causing

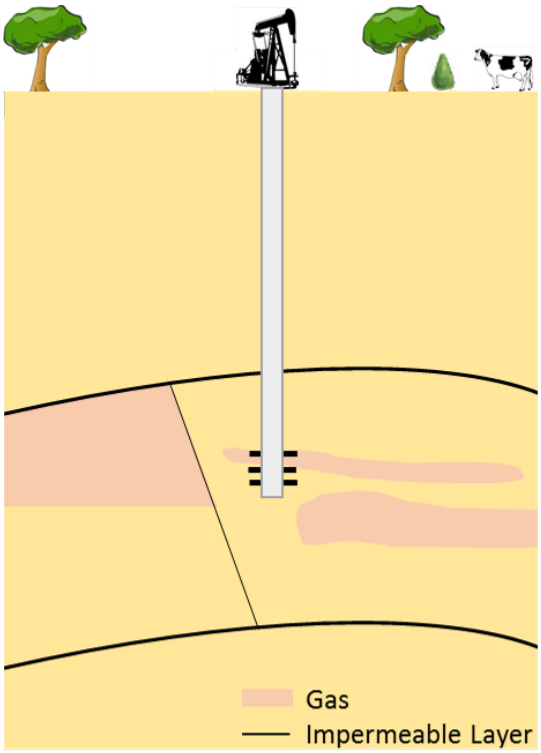


Figure 2.8: Situation before the well is hydraulically fractured. The sealing fault is obstructing the gas to flow. Another gas pocket on the right is not flowing neither.

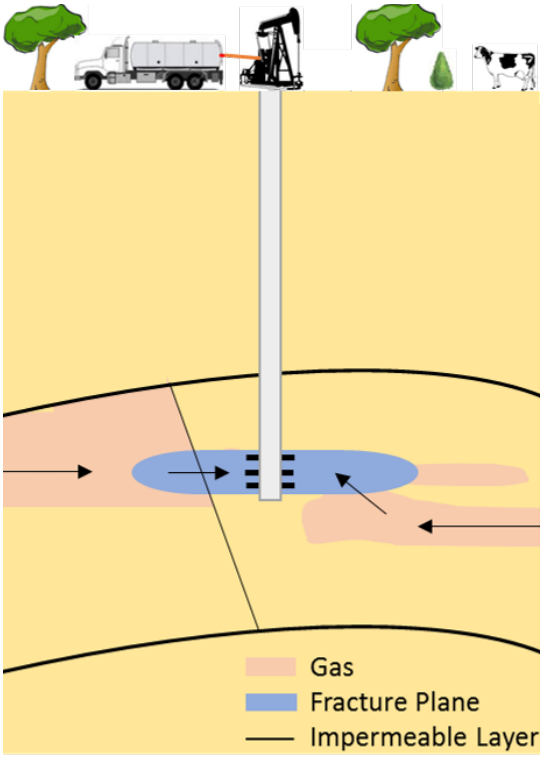


Figure 2.9: Situation after the well is hydraulically fractured. The fault and gas pocket boundaries are pierced by the fracture plane, making the gas mobile to flow.

higher risks for inducing seismicity[20]. Also the CCA came up with a study that concluded most experts judged the risk to be low and can be minimized by through careful site selection, monitoring and management[21].

# 3

# METHODOLOGY

The methodology can be subdivided into three phases. The first phase is the gathering of data for making a consistent model. Data used in this project is coming from operators reports and are all stored in a high level database. The second phase is the technical analysis and will be explained later on. The last phase is bringing all the information together to make an economical analysis and find trends in the output data.

## 3.1. WORKFLOW

The workflow to make a technical analysis for a fractured well is summarized in five steps:

1. Determine the Liquid Loading Rate
2. Perform Decline Curve Analysis
3. Perform Material Balances
4. Build Analytical Model by execution of a history match
5. Make a Forecast

The first step is to determine the liquid loading rate via the Turner or Coleman rate. This will be explained in section 3.2. The software package IHS Harmony is used for the steps two till five. The analytical model is made with rate transient analysis and will be explained in the sections 3.3 and 3.4. Based on this technical analysis, the economic evaluation is described in section 3.5. Lastly, the assumptions made in the methodology are explained.

The hydraulic fractured wells could be divided into two groups. The first group is the wells that are fractured after they have produced for a certain period. These wells have pre and post frac data. The other group consists of wells that are immediately fractured, due to disappointing well tests or even non-flowing wells. These wells do not have pre frac data. Both groups are depicted in figure 3.1. The blue rectangles indicate the steps, the orange ellipses are in- or output variables and the diamond shape stands for the model from scratch, made without history match.

On the left hand side the first group is shown. The daily flow and pressure data are divided into the pre and post frac stages. Completion and reservoir properties are found in completion, core and well test reports and used as input parameters. The first step is to make a flowing material balance to determine the gas initially in place. This output parameter is used to make a history match. The history match is made by only changing the permeability and skin (and in case of post frac data also the half length of the frac). However, the permeability is constant in both pre and post frac data, resulting in exactly the same reservoir properties. If the history match is correct, a forecast is performed. On the right hand side in the second group is shown. Since there is only post fracture data, there is only a matching procedure with these data, via the same steps as explained before. With the output parameters determined in the analytical model, it is possible to develop the model from scratch. This model is built on the same completion and reservoir parameters, and the GIIP and permeability output of the model with frac. Assumed is the skin to be zero in all these cases to get a consistent model.

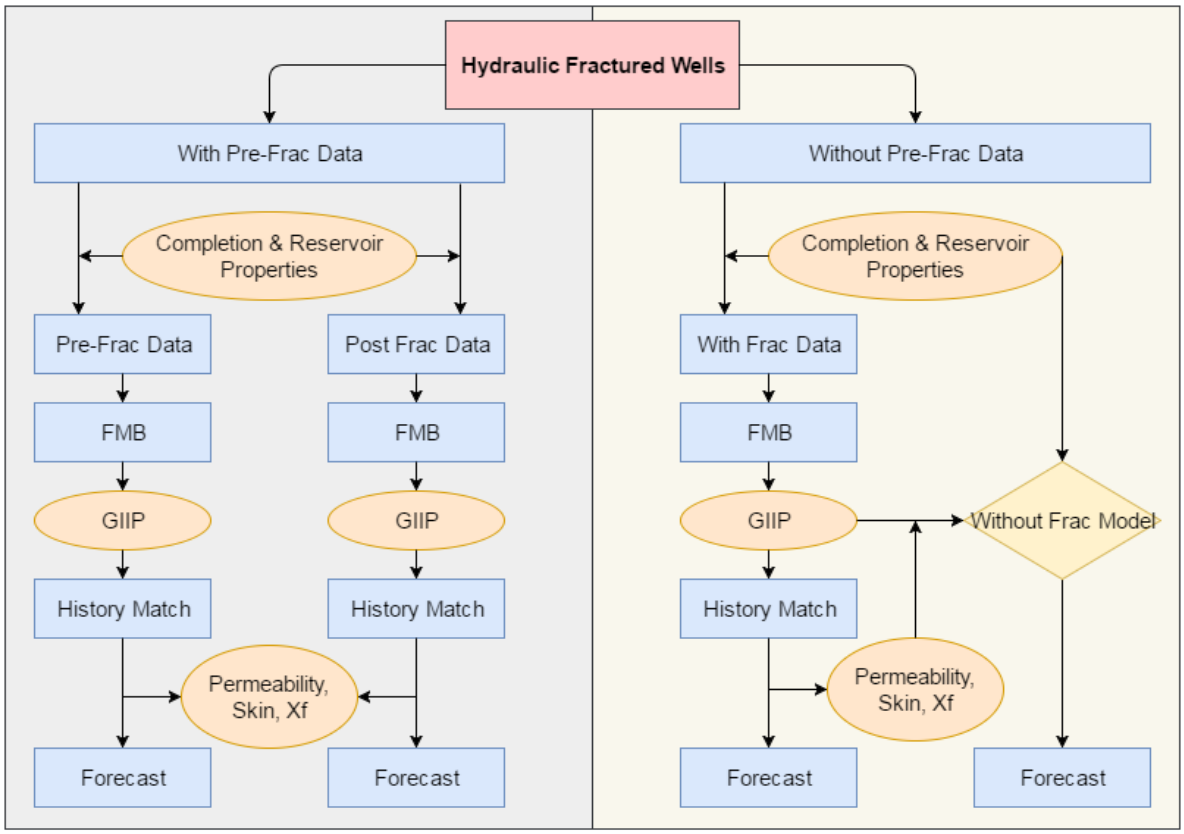


Figure 3.1: Workflow of the project. The blue rectangles represent steps, the orange ellipses are in- and output variables and the diamond shape stands for the model from scratch, made without history match.

## 3.2. LIQUID LOADING RATE

Liquid loading is an important cut-off criterion for forecasts of gas wells. Nearly every gas well will suffer from liquid loading at some point in its production life. When reservoir pressures drop, gas velocities become too low to transport liquids to the surface. Operators try to avoid this problem by implementing end of field life techniques. Examples are installation of velocity strings, foam injections or plunger lifters. However, these techniques are quite expensive and the outcome is not always certain. The first attempt to continue production is by huff 'n puff production. The well is shut-in for a certain period and hereafter produced for a certain period. During the shut in period, pressure builds up. When re-opening the well, the well is able to produce again and lift liquids to surface[22]. The discontinuous production behavior is causing problems with history matching within IHS Harmony. The software is not capable of handling the huff 'n puff behavior when liquid loading occurs. To avoid this problem the liquid loading rate is calculated via the Turner or Coleman methods. The calculated critical flowrates with their associated flowing tubing head pressure are limitations for the history matching and forecasting procedure.

The theory is based on a droplet suspended in the flowing gas stream, where two forces are acting on it. The drag force is pushing the droplet upwards and is generated by the flowing gas, while the force of gravity is pulling the droplet downwards. The gas rates exceeding critical velocity are predicted to lift the droplets upward. Lower rates allow droplets to fall and accumulate. Based on experiments Turner developed the critical velocity equation presented in (3.1)[23].

$$v_{gc} = 1.92 \frac{\sigma^{\frac{1}{4}} (\rho_l - \rho_g)^{\frac{1}{4}}}{\rho_g^{\frac{1}{2}}} \tag{3.1}$$

where $v_{gc}$ is the critical gas velocity $[m^3/s]$, $\sigma$ is the surface tension of liquid to gas $[dynes/cm]$ and $\rho$ stands for the liquid and gas density in $[kg/m^3]$. The theory does not describe the real mechanism, but it is a practical determination of the critical velocities. Coleman developed a similar formula, but with a difference

in the first term, which is assumed to be 1.52. This resulted from data for wells with lower well head pressures than those tested by Turner[24]. This leads to a lower critical flowrate compared to the Turner rate. The $\rho_g$ is calculated via (3.2).

$$\rho_g = \frac{2.699\gamma_g P}{TZ} \tag{3.2}$$

The critical velocity calculated with (3.1) is converted into the critical flowrate with the ideal gas law. The Z-factors are calculated with the Beggs- and Brill correlation and is explained in Appendix A.0.1. According to equation(A.9) and (A.22), the critical flowrate is influenced by the impurity composition of the gas and the surface where the gas flows through. In this case this means the inner area of the tubing. The influence of both parameters on the critical flowrate can be seen in figure 3.2.

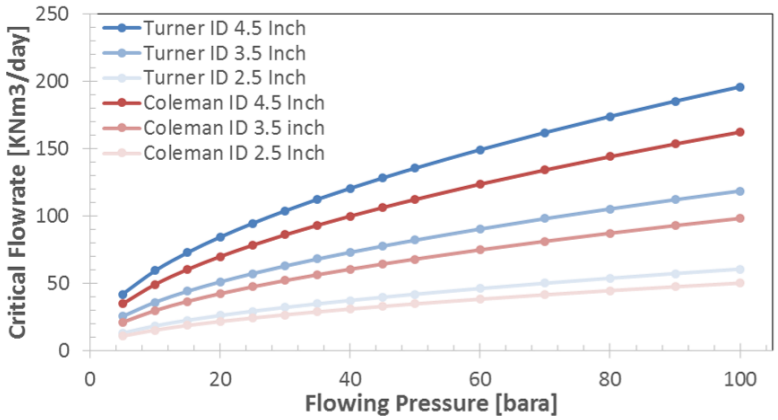


(a) Influence Inner Diameter on Critical Flowrate

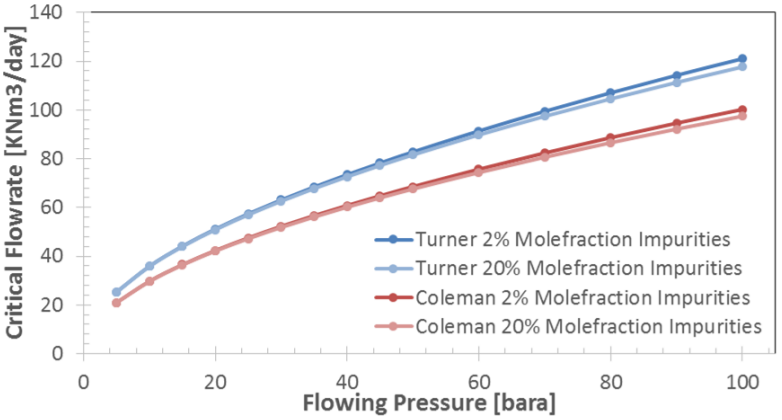


(b) Influence Gas Composition on Critical Flowrate

Figure 3.2: Turner- and Coleman Correlations

The critical flowrate is determined for a range from 5 to 100 bar flowing well head pressures. In this study, a flowing tubing head pressure of 15 bar is used. According to a research project of Siemens AG, there are three typical stages within the production process [25]. The first is the free flow stage. The well flows with a wellhead pressure between 100 and 300 bar and there is no compression needed. Phase two begins when the wellhead pressure becomes lower than 80 bar and central compression is installed. The last phase is when the reservoir pressure is low and the wellhead pressure becomes lower than 10 bar. This is the moment Siemens installs the wellhead compression to prevent liquid loading problems. To avoid this stage, this study is only focusing on the production before the wellhead compressors are installed, until 15 bar FTHP.

## 3.3. DECLINE CURVE ANALYSIS

Although there are a lot of modeling methods to determine production behavior nowadays, decline curve analysis is still the most used. It is a useful- and frequently accurate analysis technique when properly applied. Decline analysis is the empirical technique to extrapolate trends in the production data. Its purpose is to generate a forecast for future production and it is capable of determining ultimate recovery factors. The production rate relationships are developed by Arps back in 1956[26]. The general decline curve equation is given in (3.3).

$$q = \frac{q_i}{(1 + bd_i t)^{\frac{1}{b}}} \tag{3.3}$$

where:

| | | |
|---|---|---|
| q | = | flowrate $[m^3/s]$ |
| $q_i$ | = | initial flowrate $[m^3/s]$ |
| $d_i$ | = | nominal decline factor $[s^{-1}]$ |
| t | = | time $[s]$ |
| b | = | hyperbolic decline constant $[-]$ |

The hyperbolic decline constant $b$ varies between 0 and 1,

$$b = \begin{cases} 0, & \text{if exponential decline} \\ 0 < b < 1, & \text{if hyperbolic decline} \\ 1, & \text{if harmonic decline} \end{cases}$$

The exponential decline will give the lowest ultimate recovery. Since the b-value is equal to 0, a linear line will be constructed. For the harmonic decline the highest ultimate recovery will be estimated, since a b-value of 1 will construct an exponential line.

The decline curves are constructed on the last production rates. This ensures the curves are drawn in the pseudo steady state regime instead of the transient state. During transient time the decline rates are normally very high, resulting in too pessimistic forecasts. Boundary dominated flow, which occurs in the pseudo steady state regime, is declining much slower than the transient flow and gives a more reliable forecast and ultimate recoveries.

The decline curve analysis is used in this study to get an indication of the GIIP. It ensures a range of the actual volumes in place which is very useful by determining the dynamic GIIP with the material balances. In addition, DCA is used as a quality check to determine the forecast predicted by RTA makes sense.

## 3.4. RATE TRANSIENT ANALYSIS

The analysis is done in IHS Harmony, which allows detailed modeling of hydraulic fracture behavior via rate transient analysis. For this study the material balance, history match and forecasting methods are used. For describing reservoir performance, rate transient analysis can be applied in the boundary dominant flow environment after the well has already produced in transient regime period in early stage of production. A lot of parameters are needed as input to perform a proper calculation of the sandface pressure. Since most of the time the data is gathered at the surface (no downhole gauges were installed), the pressures need to be converted to downhole measures. The properties needed to develop the model are summarized in table 3.1. Some assumptions have been made in this model and can be find in section 3.6.

Table 3.1: The properties needed to develop the model in IHS Harmony

| **Property** | **Items** |
|---|---|
| Petrophysical Parameters | Net Pay Height, Porosity, $S_w$, $S_g$ |
| Gas Properties | Amount of $CO_2$, $H_2S$ and $N_2$, Gas-Gravity |
| Reservoir Properties | Initial Temperature and Pressure |
| Well Schematic | Completion, Deviation and Perforations |
| Daily Production Data | Wellhead Pressures and Flowrates |

### 3.4.1. MATERIAL BALANCE

The first parameter which have to be determined is the Gas Initially In Place (GIIP) and is done with the material balance in RTA. Although this analysis is very simple, it gains insight of the overall behavior of the field and is essential to make a good history match. There are two types of material balances used in the project: the static- and flowing material balance. The static material balance is derived from the ideal gas law, and built on the assumption that all reservoirs are produced only by depletion without compaction drive or water influx. Static buildup pressures are needed which are measured during well tests. The initial downhole volume remains the same during production, so the volume at the start of the process is equal to the volume after production. This is displayed in equation 3.4.

$$\frac{G_i}{E_i} = \frac{G_i - G_p}{E} \tag{3.4}$$

where $G$ stands for the volume of gas in $[m^3]$and $E$ is the expansion factor of the gas $[-]$. The expansion factor $E$ is a relationship for relating gas volumes in the reservoir to the produced volume at standard surface conditions and is given by equation(3.5). The expansion factor is associated with the gas formation volume factor $B_g$.

$$E = \frac{1}{B_g} = \frac{V_{sc}}{V_r} \tag{3.5}$$

Combining equations 3.4 and 3.5 as explained in appendix A.0.3, will result in the following equation:

$$\frac{p}{Z} = \frac{p_i}{Z_i}\left(1 - \frac{G_p}{G_i}\right) \tag{3.6}$$

where $p$ is the pressure $[Pa]$, $Z$ the gas deviation factor $[-]$, $G_p$ the produced gas volume $[m^3]$ and $G_i$ the initial gas in place volume $[m^3]$. The Z-factor is calculated with the Benedict-Webb-Rubin equation and is given in equation(A.11) in Appendix A.0.2. This formula is distracted from the Beattie Bridgeman equation of state and is the default method to define the Z-factor in IHS Harmony.

The flowing material balance is built on flowing pressures and rates. The well does not have to be closed-in to measure static pressures. The FMB is only valid when flow has reached boundary dominated flow. Boundary dominated flow ensures the pressure decline is equally everywhere within the reservoir over time. The pressure-distance is visualized in figure 3.3.

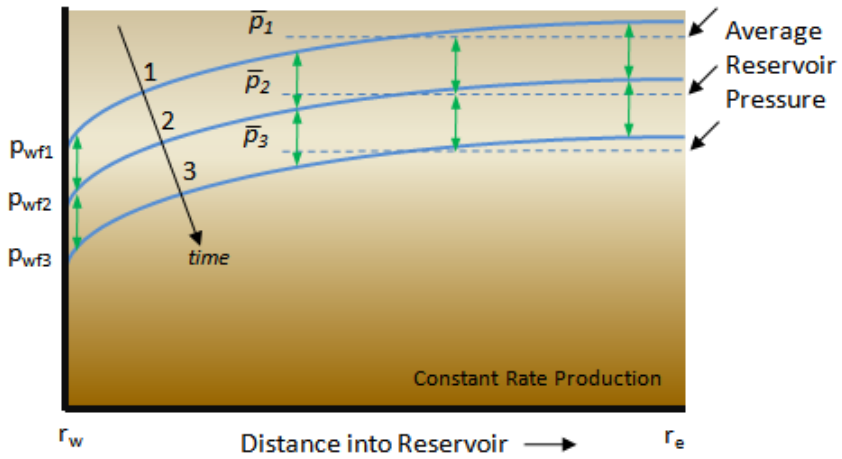


Figure 3.3: Schematic overview of pressure distribution in the reservoir when flow has reached boundary dominated flow

The GIIP is determined with the use of two methods which are coupled to each other: the variable rate flowing p/Z and the productivity index. The variable rate flowing p/Z for boundary dominated flow is calculated with the average pressure of the reservoir and is given in equation(3.7). This equation is extracted from the pseudo-steady state flow and material balance equation[27].

$$\bar{p}_r = p_{wf} + q_g b_{pss} \tag{3.7}$$

where $\bar{p}_r$ is the average reservoir pressure, $p_{wf}$ is the flowing wellbore pressure, $q_g$ the gas flowrate and $b_{pss}$ is the pressure loss due to the steady state inflow of gas. The pressure loss is assumed to be constant in time and is given in equation(3.8).

$$b_{pss} = \frac{1.147 \times 10^6 T}{kh}\left(ln\left(\frac{r_e}{r_w}\right) - \frac{3}{4}\right) \tag{3.8}$$

The productivity index (PI) is an essential part of finding the right GIIP with the FMB. The PI of a well indicates the production rate achievable under a certain drawdown pressure. The drawdown pressure is the difference between reservoir- and downhole pressure. This pressure difference is the driving force for gas flow. The productivity index in IHS harmony is modeled with the assumption the well is in pseudo steady state as well as it is in the flowing material balance. The PI-calculation is given in equation 3.9.

$$PI = \frac{1}{b_{pss}} = \frac{q_g}{p_r - p_{wf}} \tag{3.9}$$

The FMB and PI are coupled to each other by the $b_{pss}$ as seen in equation(3.7) and (3.9). Since the assumption is made that the well circumstances does not change, the productivity index has to be constant in time. This ensures the $b_{pss}$ is correct and indicates the correct GIIP.

### 3.4.2. HISTORY MATCHING

The history match is made for both the unfractured as the fractured model. The unfractured model simulates the pressure response within a homogeneous rectangular shaped reservoir. The well may be at any location within the reservoir, and the reservoir has no-flow boundaries. During very early times, the cylindrical source solution is used, which is followed by the Green's function solutions[28]. The result is superposed in time based on the rate history provided. The fracture model is also simulating the pressure response within a homogenous rectangular shaped reservoir produced by a vertical well, except there is also a infinite conductivity fracture within the model. This means the $F_{CD}$ is modeled higher than 50. Again the reservoir has no-flow boundaries and the well could be placed anywhere within the reservoir, provided that the fracture half length does not cross the reservoir boundary. During very early times, the cylindrical source solution is used, which is followed by Green's function solutions as developed by Thompson. However some slight modifications have been made within the program to simulate an infinite-conductivity fracture for a vertical well. The result is superposed in time based on the rate history provided.

To conduct our history match, some assumptions are made. The only parameters that have been changed to match the calculated pressures with the measured pressures, are the matrix permeability, skin and GIIP. However, this GIIP has to be in line with the GIIP found in the FMB. The matrix permeability in the reservoir is the same for the unfractured and fractured model, since reservoir permeability does not change by fracturing. In the fracture model the fracture half length can also be changed to find a good history match. However, this parameter is fixed since the half length of well reports is used, as described in section 2.1.

### 3.4.3. FORECASTING

The forecast is dependent on the imposed pressures and the critical flowrate. The critical flowrate is calculated with the Turner and Coleman rate as explained earlier. For forecasting there are two options in IHS Harmony to control the wellhead pressures: ramp- or step interpolation. With ramp interpolation, the initial and final wellhead pressure have to be given for the forecasting period and the program will linearly decrease the pressure at the wellhead. The step interpolation will forecast with a given constant wellhead pressure. To determine which interpolation gives the most secure forecast, three scenarios have been investigated:

- Ramp interpolation - FWHP from 100 bar to 15 bar
- Step interpolation - FWHP from 100, to 50, to 15 bar
- Step interpolation - FWHP constant 15 bar

The limitations of the chosen FWHP are 100 and 15 bar. The upper limit is determined by the Siemens compression report, where suggested that free flow occurs until FWHP of 100 bar. Since the critical flowrate is calculated at 15 bar, this is the lower limit. The step interpolation for the second case is associated with the flowrate. After discussion with professionals working at EBN, the following flowing regimes have been chosen:

- FWHP 100 bar until $q_g < 400.000\ m^3 d^{-1}$
- FWHP 50 bar until $q_g < 200.000\ m^3 d^{-1}$
- FWHP 15 bar until $q_g > q_{crit}$

In figure 3.4 the different FWHP with their effects on the forecast scenarios are given. It is clear that the ramp interpolation gives the lowest production rate compared with both step interpolations. As a side effect of this lower production rate, the abandonment rate will come later in production life. The difference between the two step interpolations is almost negligible. The constant FWHP of 15 bar is a bit more productive in the beginning, but on cumulative scale it is almost the same.

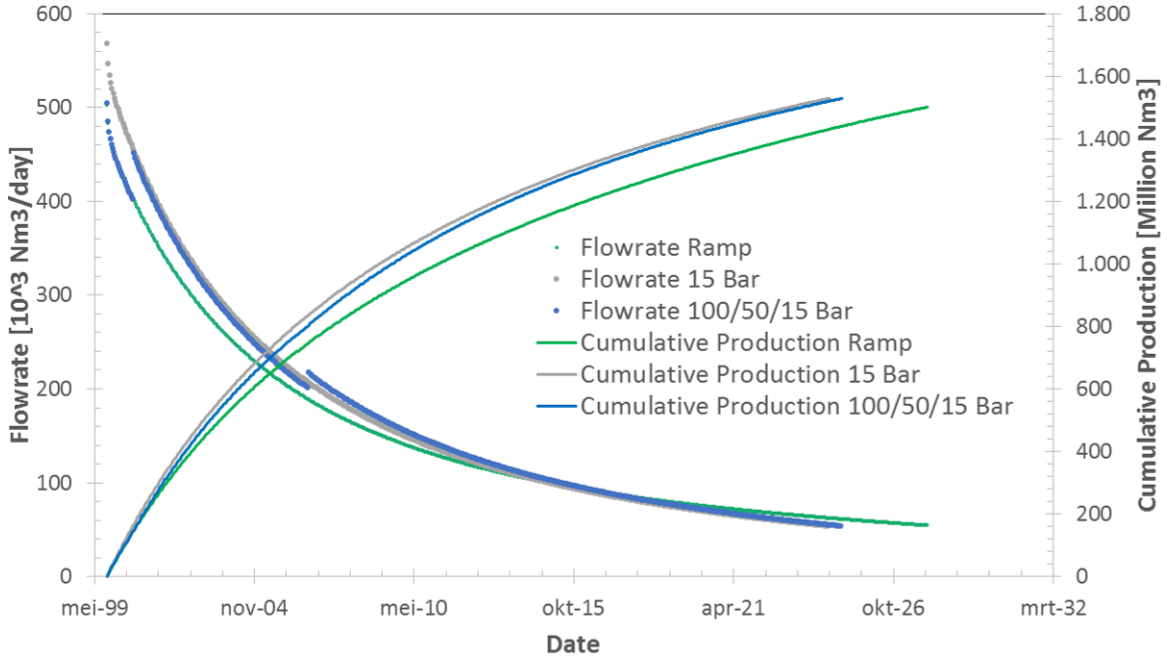


Figure 3.4: Influence of the FWHP on production rates

Although all forecast methods have advantages, the constant FWHP of 15 bar is chosen as the forecasting pressure. Firstly it is applicable to all the wells investigated. The wells which are already producing under 100- or 50 bar could not properly be described with the other step interpolation method. Secondly, the constant FWHP of 15 bar gives the full production capacity from the beginning onwards. This is not the case for the other interpolations, resulting in too positive absolute net present values.

## 3.5. NET PRESENT VALUE ANALYSIS

The Net Present Value (NPV) of the project is a measure of the economical success of the investment and is calculated with equation(3.10). In this project the used investment costs are from the well or frac proposals, also known as the Authorization For Expenditures (AFE). These are used since the realized costs were not available for a large amount of the wells. However, for six wells in the portfolio, the AFE costs were not available. Based on the costs of other fractures, an assumption of 10% of the total AFE of the wells is taken as the cost for a single fracture. The NPV is defined as:

$$NPV = -C_0 + \sum_{i=1}^{T} \frac{C_i}{(1+r)^i} \tag{3.10}$$

where $C_0$ is the investment, $r$ stands for the discount factor (in every case 8%), $i$ stands for year and $C_i$ is the cash flow for a certain year and is calculated by:

$$C_i = \Delta Q_i \times P_i \times 3.6 H_g \tag{3.11}$$

Where $\Delta Q_i$ is the difference in cumulative production between with and without fracture for a year $i$, while $P_i$ is the gas price in €/kWh and $H_g$ is the specific caloric value for gases in $MJ/m^3$. This value is determined for every field in The Netherlands by the amount and composition of hydrocarbons within the gas. The factor 3.6 is the conversion from $kWh$ to $MJ$. In figure 3.5 an example of determining $\Delta Q_i$ is shown. The gasprice and its forecast is based on the TTF spot price [29] and is given in figure 3.6.

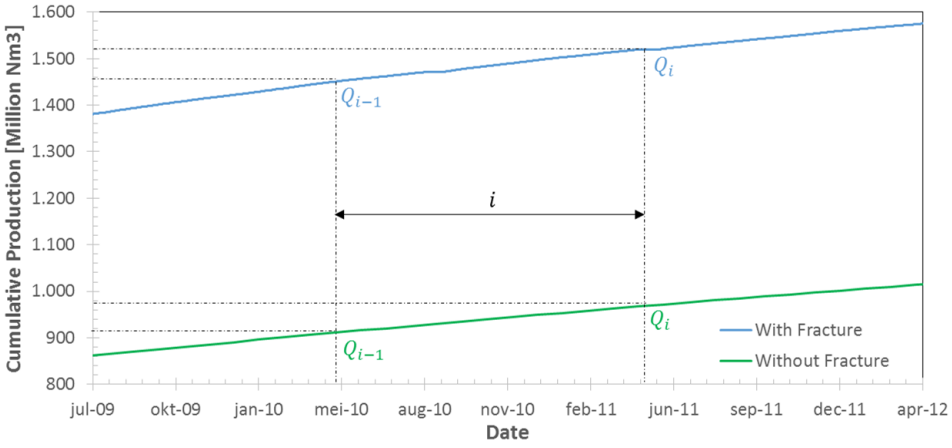


Figure 3.5: The determination of $\Delta Q_i$

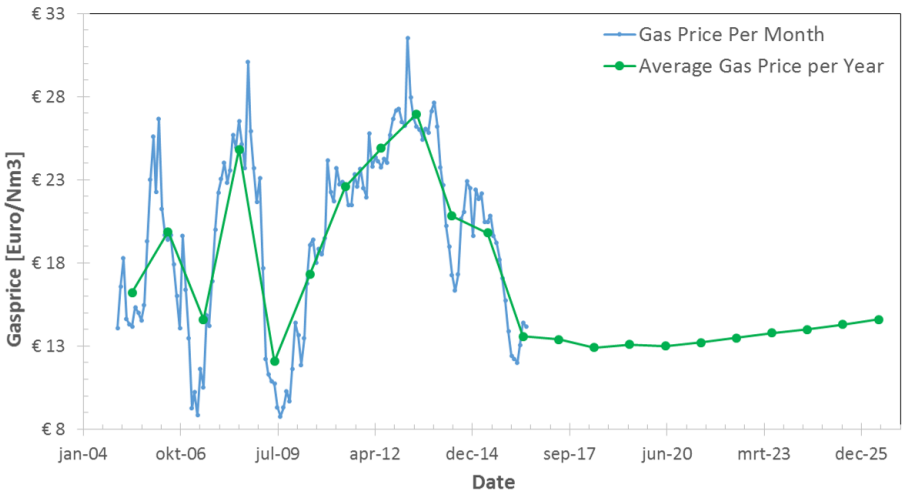


Figure 3.6: The gasprice over the years with a forecast used in this project

## 3.6. ASSUMPTIONS

The assumptions made in this project are summarized in this section. The assumptions are categorized in two subsections, being:

1. Analytical Model

   - The fracture has infinite conductivity, since IHS Harmony is not capable of modeling finite conductivity in vertical fractured well models. This leads to linear instead of bi-linear flow around the wellbore.
   - The analytical model without fracture is built on the wells that were hydraulic fractured immediately, and assumed is that all models have a skin of 0.
   - Reservoirs are produced only by depletion without compaction drive or water influx.

- The pressure within the reservoir has reached boundary dominated flow, which ensures pressure decline is equally everywhere.
- Water and condensate production is ignored in this study, since it is not properly measured by operators during production. Therefore, production forecasts are predicting until critical rate determined by Turner equation.
- When a well was already producing in critical flow regime or with FWHP below 15 bar, this part of production is ignored.
- For wells that are exhausted before critical flow rate determined by Turner is reached, are having a critical flowrate determined by end of production.

2. Economic Model

- For the fracturing costs the Authorization For Expenditures (AFE) is used, since it was hard to obtain the actual costs associated with the treatment. However, for some wells fractured immediately, the costs for fracturing are undefined included in the total AFE of well proposals. For these cases, 10% of the total AFE is used as fracturing costs.
- The gasprice has been recorded since 2005. The predicted future gasprices are determined by EBN B.V. and are predicting until 2026. Economic analysis for production profiles before 2005 are calculated with the average gasprice of 2005, while forecasts after 2026 are calculated with the average gas price of 2026.
- Discount rate is taken as 8%. This is a rule of thumb by evaluating gas projects in The Netherlands.
- Converting Guilders to Euro's is always done by 2.2:1 ratio

# 4

# ANALYTIC MODELING

In this chapter the analytical models used in IHS Harmony are presented. The decline curve models, made in this study to estimate the ultimate recovery factors, are firstly discussed. The recovery range determined with the DCA, is used as a quality check of the RTA model. Hereafter the GIIP estimation is explained by use of both the static and flowing material balance. With this estimation a history match can be performed to make a forecast.

## 4.1. DECLINE CURVE ANALYSIS

Decline curve analysis is the first analysis performed on every well. The exponential, hyperbolic and harmonic declines are used. The hyperbolic decline in this study has a standard b factor of 0.5. The results from one of the investigated wells is given in figure 4.1. The left decline curve is the exponential, while the right curve is the harmonic. The curves are drawn till the liquid loading flowrate occurs, which is calculated with the Turner rate and indicated by the green dashed line. In this particular example it can be seen that the

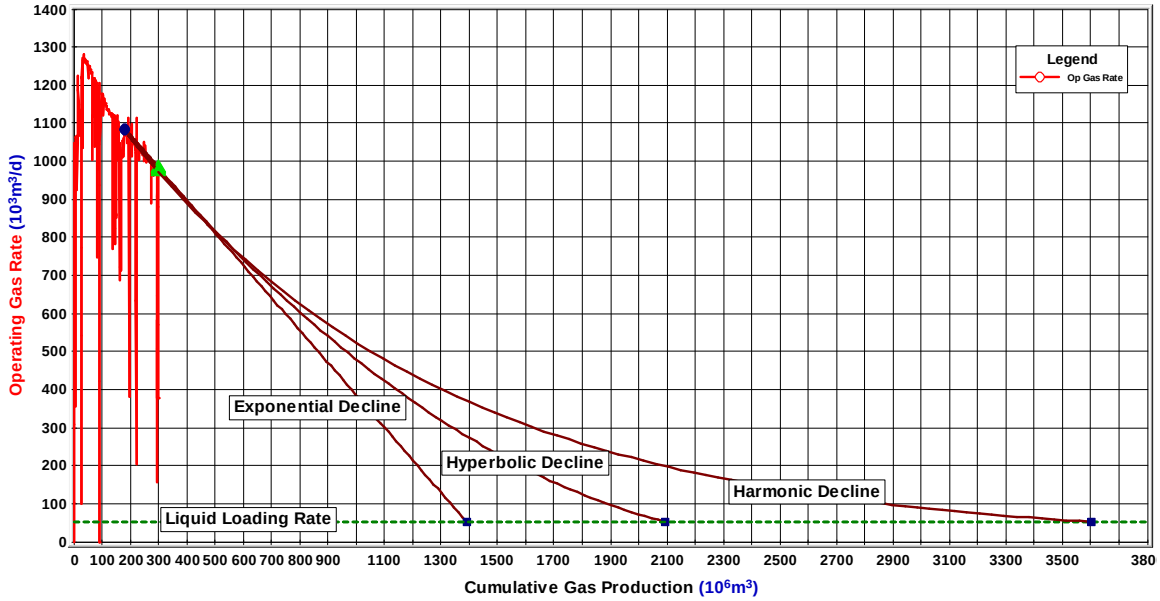


Figure 4.1: The three decline curves used in this study. The green line indicates the liquid loading rate

difference in cumulative production between the exponential and the harmonic decline is enormous. The reason is that the operating gas rate is still quite high (almost 1 million $Nm^3/d$) compared to the critical rate. If the production rate is closer to the liquid loading rate, the decline curves are having less space to diverge. This will lead to a much more precise forecasting range by decline curve analysis.

## 4.2. MATERIAL BALANCE

The material balance is made for both static as flowing pressures as long as the data was sufficient. Especially the pressure points necessary for the construction of the static material balance were often not found, since it is expensive to shut in the well for only conducting pressure measurements. The flowing material balance is made for every particular well since there was enough data and it was given the best estimation of GIIP. In figure 4.2 both the static as the flowing material balance can be observed. In this figure, the gray colored data on the left hand sight of the graph, are the data points before the well was fractured. Therefore, they are ignored in this particular analysis. The hydraulic fracturing was executed when the cumulative production was almost 40 million $Nm^3$. The green diamonds are indicating the productivity index. As explained in the methodology, it is necessary to construct a productivity index line through the data which is as flat as possible to get a proper Gas Initially In Place determination. The constant Productivity Index can be well observed in this case. An observation that immediately stands out is that the productivity index of this well increases tremendously after stimulation. The PI is below one before the fracturing treatment and afterwards it is almost four. Although the PI-values are not that high, it gives a good indication of what for impact a hydraulic fracture could have on the increment of production. Furthermore the static p/Z points are indicated by the red circles. The first point can be seen at the beginning of production. This pressure point is equal to the initial reservoir pressure. The second one is almost invisible, but is located after 150 million $Nm^3$ of production. The purple squares represent the flowing p/Z points. To get a proper GIIP estimation, both the static as flowing p/Z point should lie on the blue linear line while the productivity index is constant. That gives in this example a GIIP of 410 million $Nm^3$. This property is an important parameter for making a history match, and therefore need to be determined accurately.

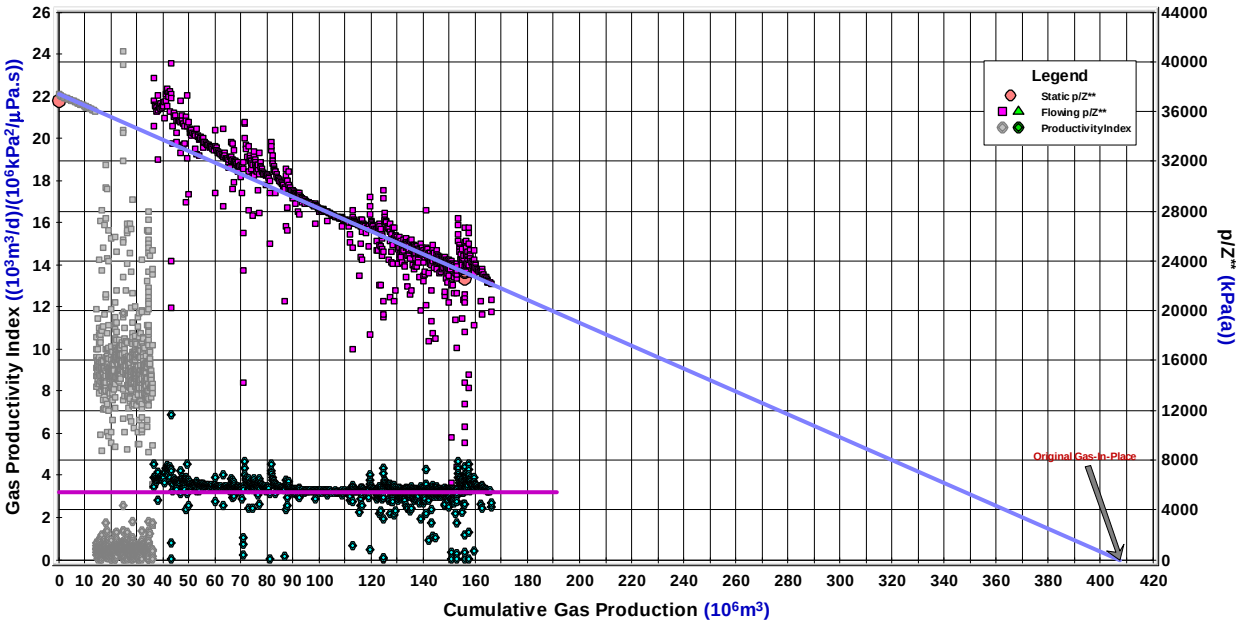


Figure 4.2: The material balance for both the static- as the flowing case. The red circles are the static p/Z points, the purple squares are the flowing p/Z points and the productivity index is given in green colored diamonds. The productivity index is given in pseudo pressure units. This ensures a linear line can be constructed. Although the PI is constant, there are some outliers around the constructed PI-line. These outliers are observed after the well has been shut-in and therefore the well is producing in transient regime for a while. Therefore there could be a small uncertainty in the estimated GIIP. However, this is rectified by history matching since it is not possible to make a match with a wrong GIIP.

## 4.3. HISTORY MATCHING

One of the most important parts of modeling is making a good history match. As mentioned earlier, this is done by finding the right permeability, skin and GIIP. In figure 4.3 two history matches of the same reservoir are shown. The red squares are indicating the gas flowrates The brown circles are the calculated sandface pressures based on the originally measured flowing well head pressures during production. The most impor-

tant item in this graph is the brown line, which is the modeled pressure response calculated by the program. The pressure response is calculated on the flowrates and all reservoir/completion properties.

The history match only makes sense if this line is matching with the calculated sandface pressures. This means the reservoir properties are well chosen. If there is not a sufficient match between the calculated sandface pressures with the modeled pressure responses, the successive forecast is worthless. Since the reservoir properties are determined wrongly in that case, the reservoir depletion is also calculated incorrectly. All predicted forecasting models are associated with the reservoir pressure. In figure 4.3(a) an example due to a wrongly chosen permeability is given (too low), while the permeability of the model in figure 4.3(b) is such that it lead to a good match. Furthermore, the blue line represents the simulated reservoir pressure which is slowly depleting.

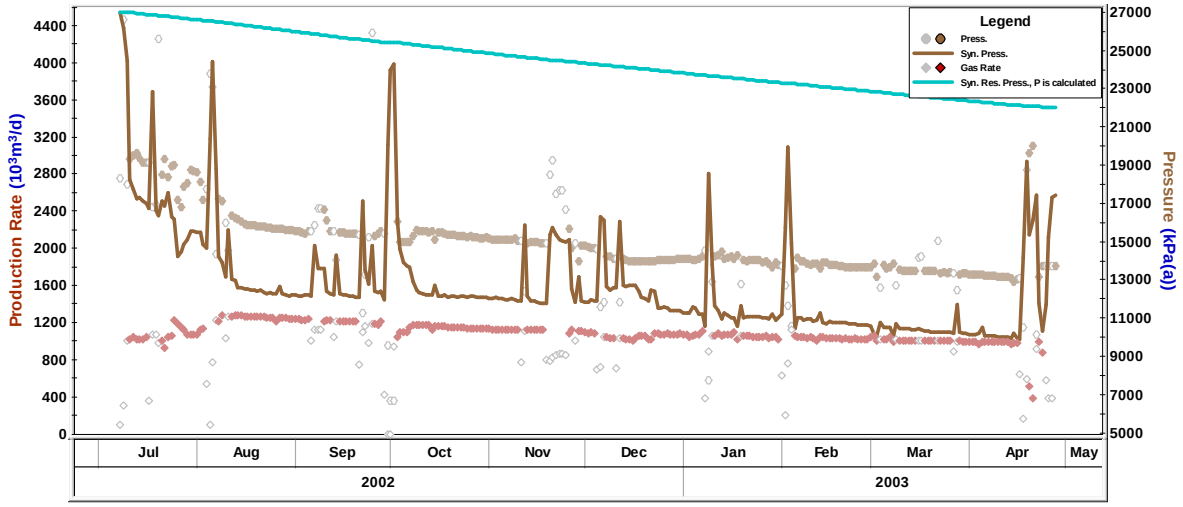


(a) Matrix Permeability 4 mD

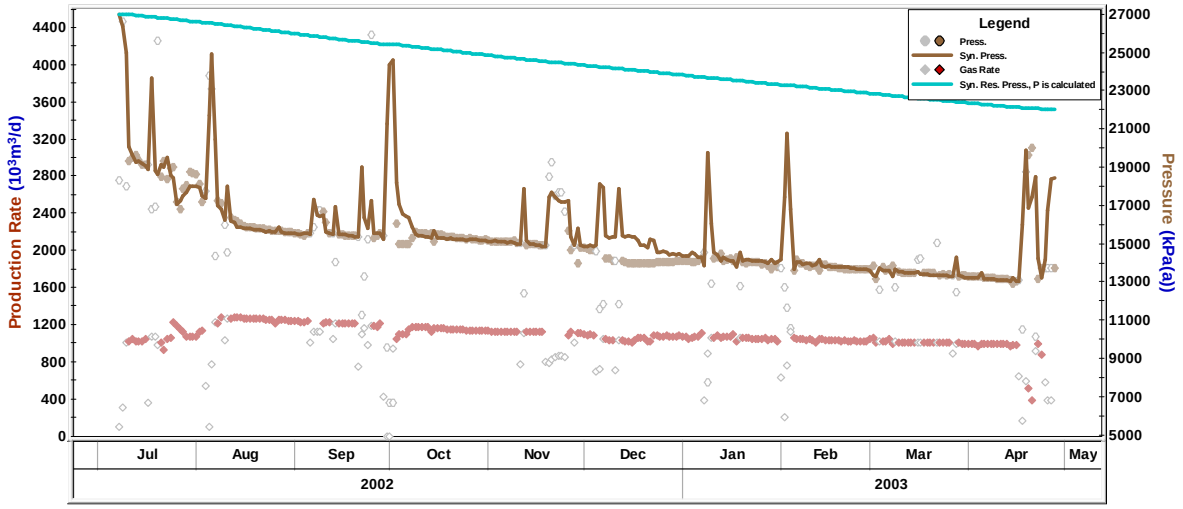


(b) Matrix Permeability 5 mD

Figure 4.3: Examples of a bd 4.3(a) and good history match 4.3(b)

## 4.4. FORECASTING

When a satisfactory history match is made, the forecast can be generated. This was done by using a 15 bar FWHP as discussed earlier. The boundary condition for the forecast is the calculated liquid loading rate reached at 15 Bar FWHP. An overview of a forecasting procedure within IHS Harmony is given in figure 4.4.

The flowrates are colored in red. The transition from real to predicted flowrates is relatively smooth, indicating the model is approaching reality. Furthermore the calculated sandface pressure is indicated by the brown line. An issue experienced during forecasting, was the implementation of downtime. There was not a user friendly way of implementing downtime in the software package. If all steps have been performed in the right

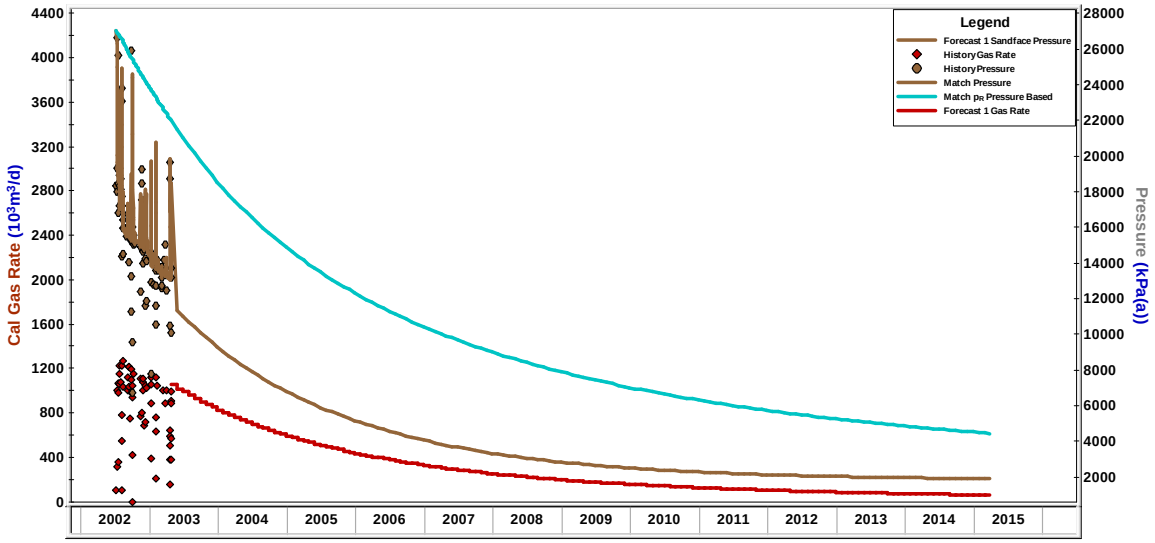


Figure 4.4: Example of a forecast in IHS Harmony. The red circles are indicating the normalized flowrates, the brown line the calculated sandface pressures and the blue line is the calculated reservoir pressure. Downtime is not included in this forecast since it is hard to implement it

way, a realistic producing profile can be constructed; an example is given in figure 4.5. This example well was fractured after a certain period, so it is having pre and post frac data. The blue dots are the original data before the well was hydraulically fractured, while the purple dots are the original data after the treatment. The stimulation took place at the vertically dotted line. Two models have been made on the production data: one before the fracture was set and one afterwards. This resulted in two different forecasts: one without frac (green dots) and one with frac (orange dots). Further, the cumulative production of both models is visible. Since it was not possible to implement the downtime easily within IHS Harmony, this is done by hand. The downtime observed in the original data after the frac, has been implemented in the forecast model without frac (green dots). This can be clearly seen in the graph by the discontinuous production. Models forecasting beyond the original data does not include the downtime, since it is not possible to determine future downtime periods.

Although the analytical model was applicable to almost all wells, there were some exceptions. The exceptions are made for five wells that are already exhausted. For these wells a different approach have been used in terms of abandonment rate. The abandonment rate of these wells were not equal to the liquid loading rate, but to the final flowrate measured before the well died. An example is given in figure 4.6. There is no forecast generated for the model with fracture since the well has already killed itself at that point. The abandonment rate is presented with a black dotted line in the graph, and is thus equal to the final flowrate before the well died.

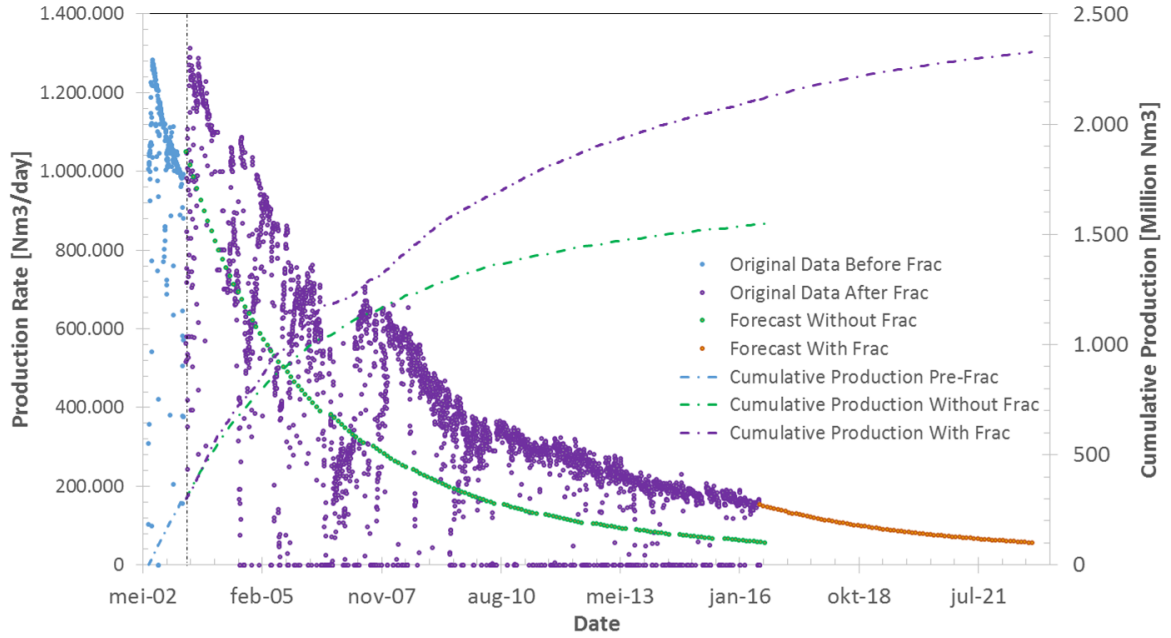


Figure 4.5: The final production profile after the five steps are conducted. The blue and purple dots are the original data: blue before the fracture and purple post frac. For both cases a model has been made and a forecast was generated. The green dots are the forecast without fracture, while the orange dots are with fracture. The fracture in this case has an enormous impact on the cumulative production.

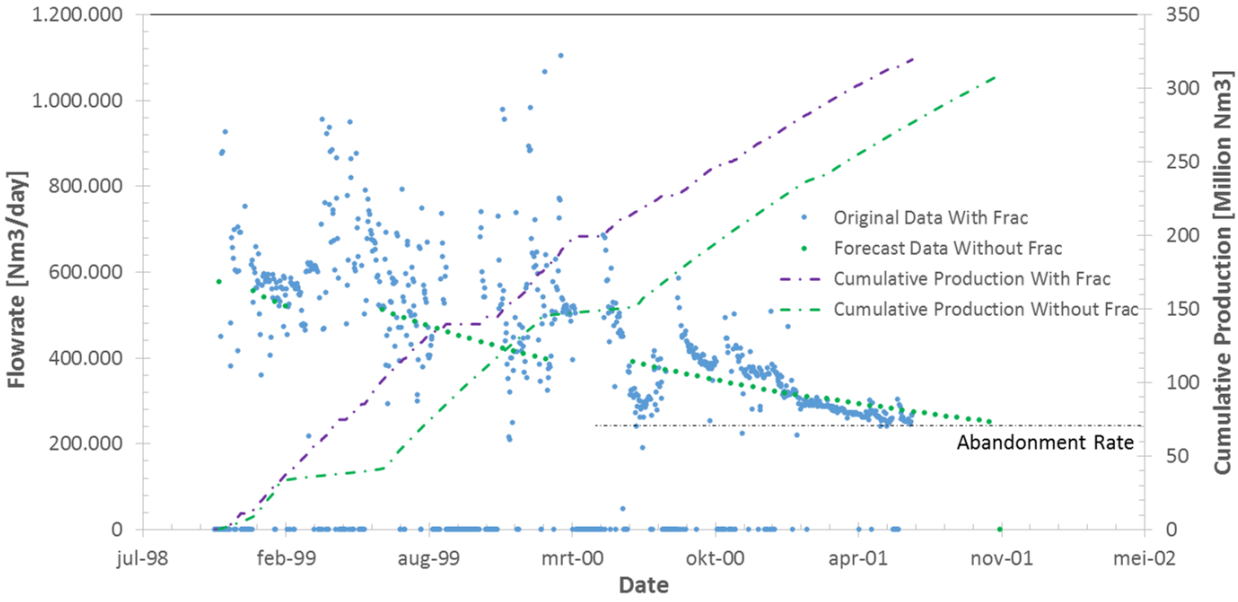


Figure 4.6: Example of forecasting a well that is already exhausted. The final rate where the well was on production before it killed itself is used as abandonment rate for the forecast without fracture. The blue dots are the original data while the green dots are the modeled production rates without fracture.

# 5

# RESULTS

In this chapter the results of the project are described. Firstly, the wells with pre- and post frac data are presented. These wells were fractured after they already produced for a certain time. This will be followed up with wells that have only post-frac data. These wells are immediately fractured due to disappointing well tests with low production rates. Both sections are describing the technical and economical analysis. To get to a proper overview, all wells are compared together in the third section. Lastly, two wells that have been subjected to failing hydraulic fracturing treatment are discussed to determine its impact on production.

## 5.1. WELLS WITH PRE- AND POST FRAC DATA

### 5.1.1. TECHNICAL ANALYSIS

The productivity index is a good measure to quantify the technical success of a hydraulic fracturing treatment. For all 19 wells that have pre-frac data, the PI is calculated and depicted in figure 5.1. The calculations are done before and after fracturing. On the y-axis the productivity index after the fracturing treatment is presented, while the x-axis is before. The different colors of the datapoints are visualizing different mesh sizes of the proppant. Three lines are drawn within the figure to indicate the incremental factor of productivity. The PI incremental factor lines are respectively: one (black line), two (blue line) and three (orange line). Finally there are five wells having a more than three times higher PI. There is only one well ranging between the two- and three times incremental factor lines. Most of the wells (12), are having a productivity increase between one and two. There is only one well that has a lower productivity index after the treatment and is classified as a technical failure. Properties associated to the increment in PI are discussed in section 5.3.

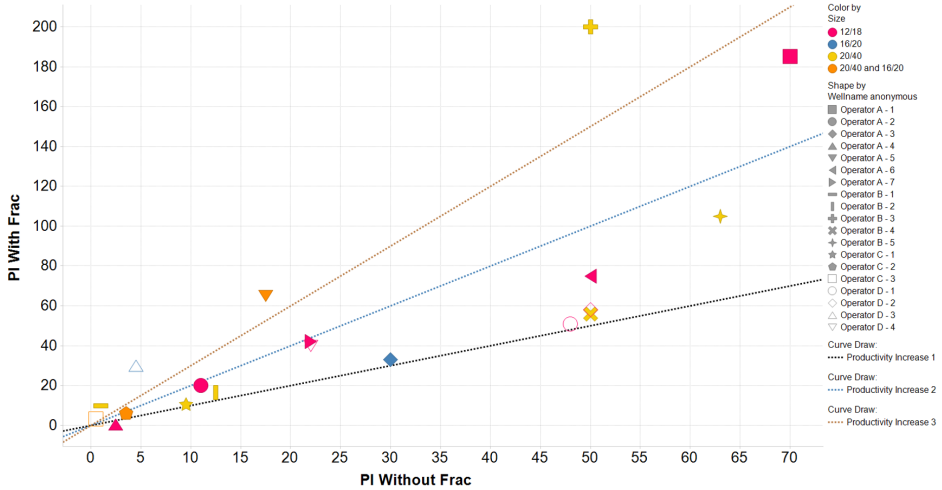


Figure 5.1: Productivity Index before (x-axis) and after (y-axis) the fracturing treatment expressed in $\frac{10^3 m^3/d}{10^6 kPa^2/\mu Pas}$. The three lines that are drawn indicate the PI incremental factor lines: the black line is no increase, the blue line is a doubling and the orange line is a tripling.

### 5.1.2. ECONOMICAL ANALYSIS

#### TIMING OF THE TREATMENT

To quantify an economical analysis, the net present value per project is calculated. Since hydraulic fracturing accelerates production, the incremental NPV is a good measure to define the success of a treatment. The first parameter that can be associated with a positive economic value, is the timing of a treatment. The earlier a treatment is conducted within a well's production life, the higher the chance of economic success. In figure 5.2 this timing, in terms of depletion of the reservoir, can be observed. It can be seen that when the reservoir pressure has already been depleted for more than 35% of its initial value, the economic outcome becomes uncertain. All eight wells that have been fractured before the reservoir pressure is depleted by 35%, are an economic success. Only two wells are having a negative net present value. Especially well A-4 is very negative, since it has been fractured too late in production life: the reservoir pressure was on 8% of its initial pressure. The constructed blue line represent the € 5,000,000 NPV-line. This arbitrary range has been chosen to give an indication of a transition zone between negative and positive values.

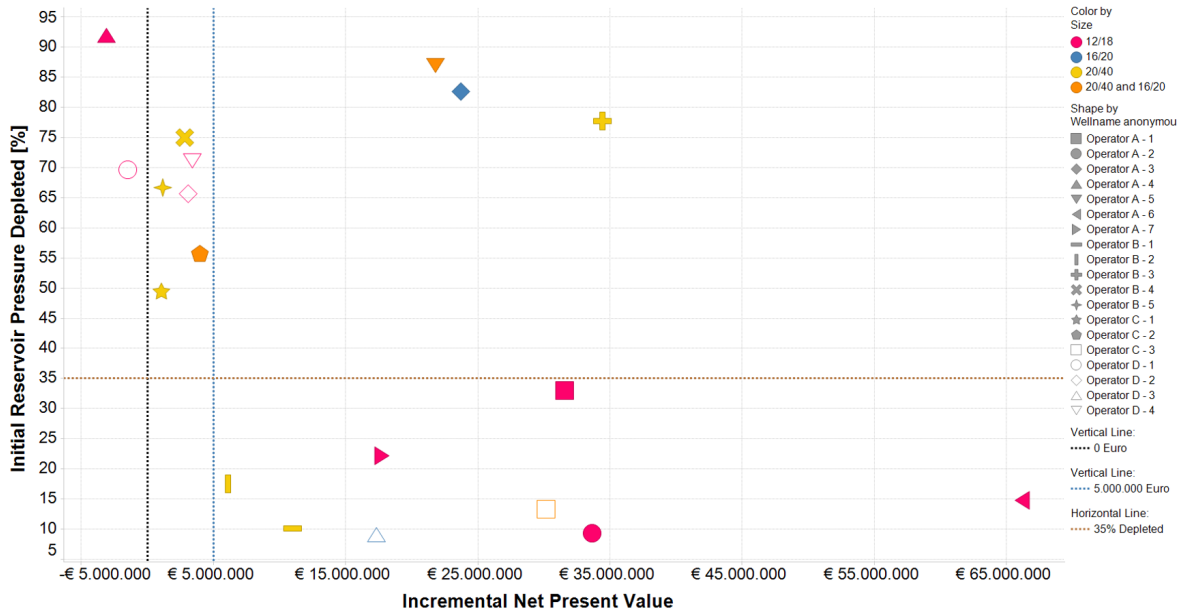


Figure 5.2: The percentage of the initial reservoir pressure that is depleted when the hydraulic fracturing treatment is executed. The black dashed line indicates the € 0 NPV-line. The € 5,000,000 line and is blue colored, and forms the arbitrary upper limit of a range of disputable successes.

In figure 5.3, the observed timing trend is expressed in volume of gas in the reservoir. The left figure is the initial dynamic GIIP before the well is hydraulically fractured. In the right figure, the volume of remaining recoverable gas in the reservoir at the moment of fracturing is visible. In this graph the symbols are varying in size. The size of the symbol indicates the percentage of gas that remains in the reservoir as part of the dynamic GIIP after hydraulic fracturing. This includes the possibly extra connected dynamic GIIP. The graph indicates that the wells located in the negative- and disputable range are having small icons and low recoverable reserves. The larger icons are all lying outside the range, except the three outliers that are discussed below.

From the wells that are fractured later in production life, three wells are positively standing out (wells A-5, A-3 and B-3) compared to the wells that are lying in the negative and disputable range. The reason can be found in figure 5.4. In this figure the PI incremental factor and extra connected dynamic GIIP are visible for the wells that are fractured later in production life. Well B-3 has a high PI incremental factor (higher than four) and connects extra dynamic gas (800 million $Nm^3$), resulting in the highest net present value of the wells that are stimulated in the end of production life. Well A-5 has also an increment in productivity, while A-3 only connects extra recoverable gas. From the graph it can be concluded that wells that are having negative NPV's, are not connecting any extra gas and the productivity did not increase (0.2 and 1.06 respectively).

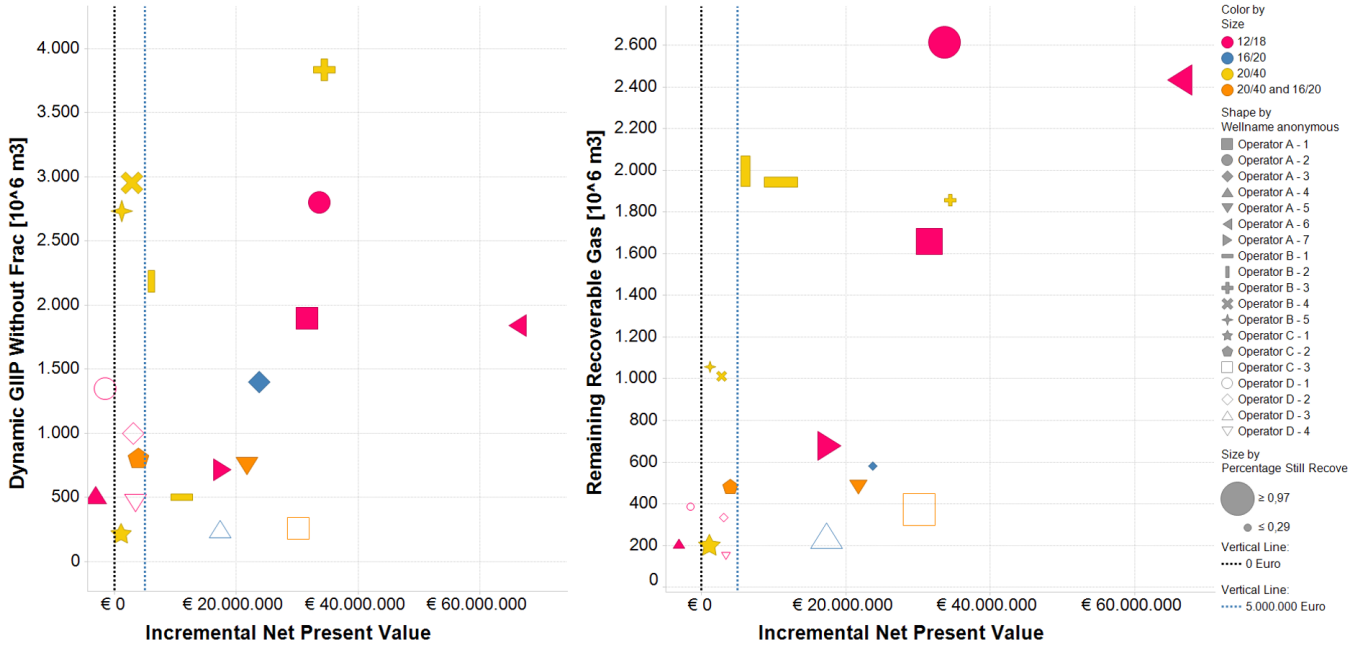


Figure 5.3: The left figure indicates the dynamic GIIP without the fracture. The right figure presents the remaining recoverable gas volume. The icons are varying in size and indicate the percentage of gas that remains in the reservoir as part of the dynamic GIIP after fracturing. A larger icon indicates a larger percentage.

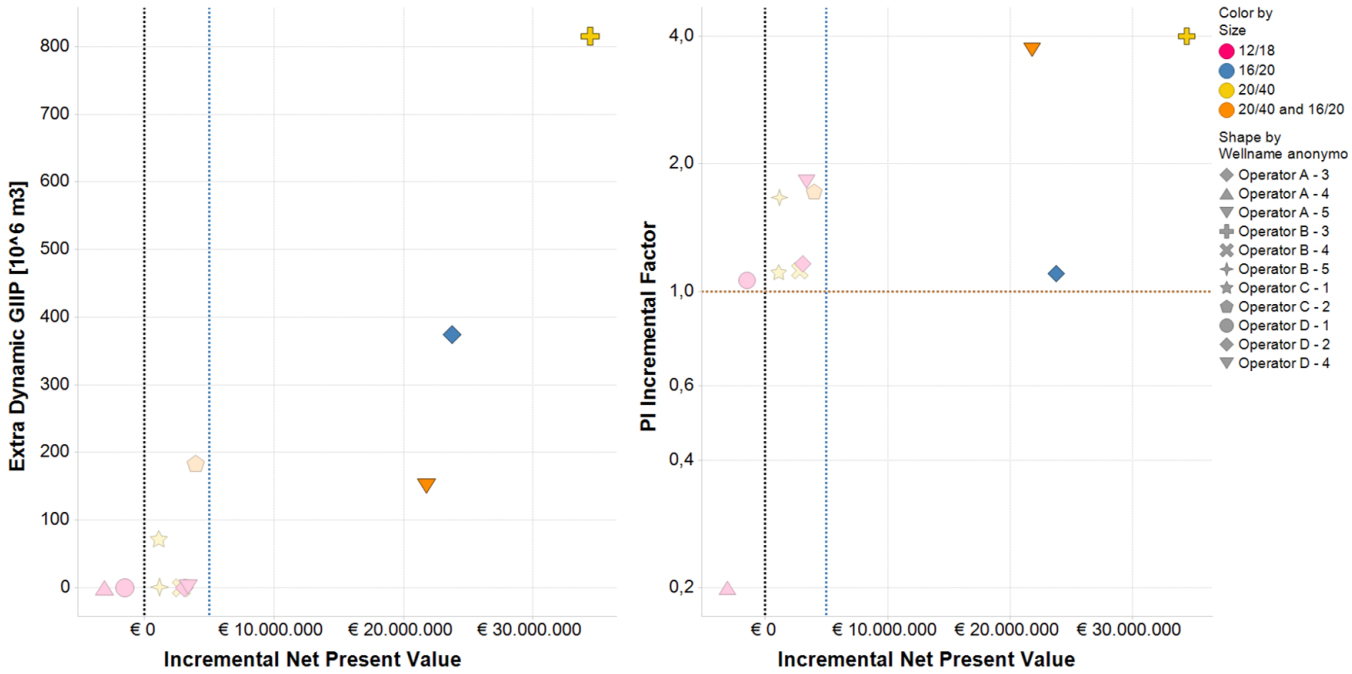


Figure 5.4: The eleven wells that are fractured later in production life (>35% of $P_r$ depleted). The three wells adding high cash values are highlighted in the figure. These wells are connecting extra dynamic gas and/or having a high increment in the productivity index.

### FRAC PROPERTIES

Besides the timing of a treatment, the properties of the fracture might determine the success. In figure 5.5 the two properties of the fracture determined in this study to be the most important, are summarized. This includes the quantity injected proppant (the left figure) and the half length of the fracture (the right figure). From the graph it can be seen that more than 100,000 kg injected proppant indicates a successful treatment. This will also be proven in the next section 5.2 by wells that do not have pre-frac data. Another trend observed in the data is indicated by the brown dashed lines. If the amount of injected proppant is lower than 70,000 kg and the half length of the fracture is equal to or lower than 50 meter, the fracturing results in a net present value lower than €5,000,000. In this case, well A-4 is assumed to be an outlier, since the fracturing job was performed while the reservoir pressure has already been depleted for 92% as explained earlier. Two good examples of the boundary ranges are wells C-3 and A-1. Well C-3 has the lowest amount of injected proppant (21,389 kg), but has still a high economic value, since the half length of the fracture is 100 meter. This ensures a long conductive path is created within the reservoir, making it easier for the gas molecules to flow. The opposite of this behavior is experienced by well A-1. This well has one of the shortest fracture lengths (47 meter), but the quantity of injected proppant is high (130,000 kg). This ensures the fracture is highly conductive and capable of transporting gas molecules faster to the well.

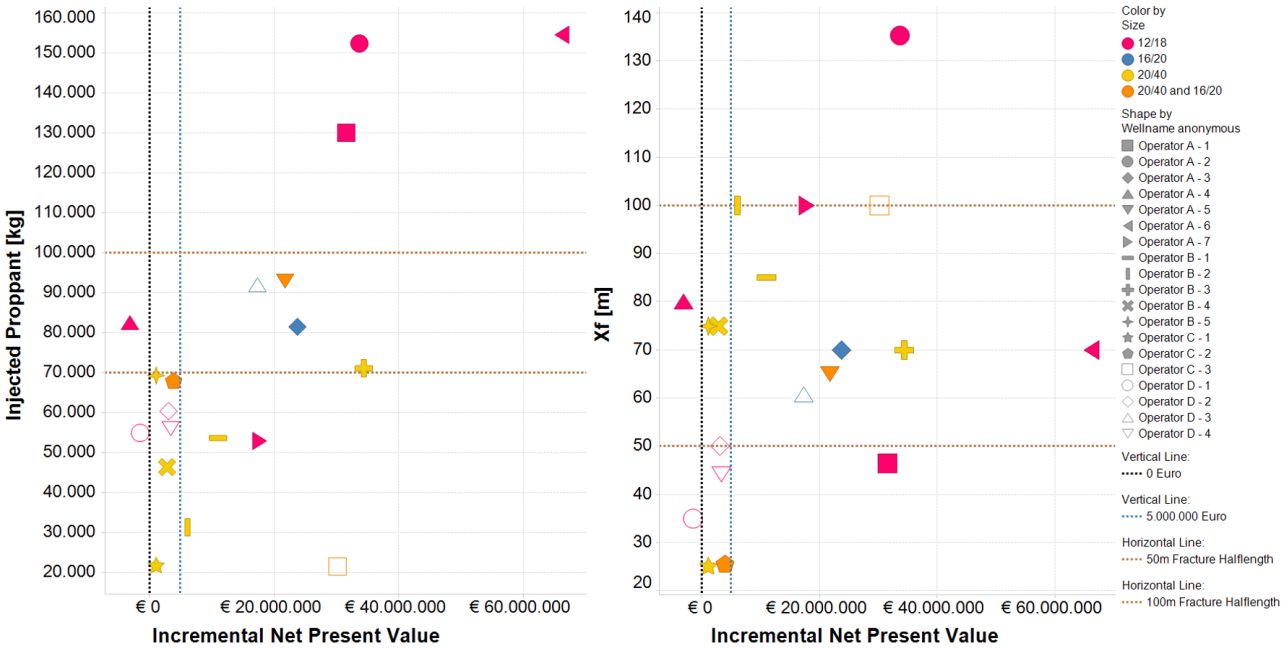


Figure 5.5: Properties of the fracture. The left figure shows the injected proppant injected during the execution. The right figure is the half length of the fracture.

Besides the already mentioned results, there are no other correlations found that can immediately assign value to the success of a fracture. Possibly, these correlations were not found due to lack of statistical data. However, all parameters investigated are summarized in figures and presented in appendix C.1. Properties investigated are including reservoir properties and treatment associated parameters:

- Permeability
- Porosity
- Pad Volume
- Injection Rate and Concentration
- Tip Screen Out

## 5.2. WELLS WITHOUT PRE-FRAC DATA

### 5.2.1. TECHNICAL ANALYSIS

The productivity indexes for wells without pre-frac data are also calculated to express the technical success of the treatments. Since there is only post-frac data available, the PI with fracture can only be determined from the flowing material balance in IHS Harmony. The PI for the unfractured model is calculated by the pressure and flowrates generated by the program. The PI values with- and without fracture are depicted in figure 5.6. In the legend, there are two wells visible including two fractures. These wells have been fractured multiple times and are having two fractures with different properties. Each fracture within a multiple fractured well is treated as an individual fracture to compare its quality with respect to the single fractures. This is done by assigning value to the fractures based on the GIIP they are connecting to. Since a double fracture is modeled as a multilayer reservoir, the two fractures are both connected to a different part of the reservoir. If the first fracture is connected to 400 million N$m^3$ dynamic GIIP and the second to 200 million N$m^3$, 2/3 of the gained value is associated to the first fracture.

The figure with productivity indexes is made in the same way as figure 5.1. The first thing that stands out from the figure, is that the PI-values are much lower compared to the reservoir with pre-frac data. This is quite logical since the wells having pre-frac data were able to produce without a fracture for a certain period. The PI for wells that are immediately fractured are generally four times lower compared to the wells that have produced without fracture from the beginning. The first conclusion based on this graph is that all investigated fracs have been a technical success, since the PI have been increased for all wells. The PI of six wells have been increased more than three times and are lying above the orange dotted line. Eight wells have been encountered an increase between the two and three, while PI of the other three wells increased by a factor between one and two.

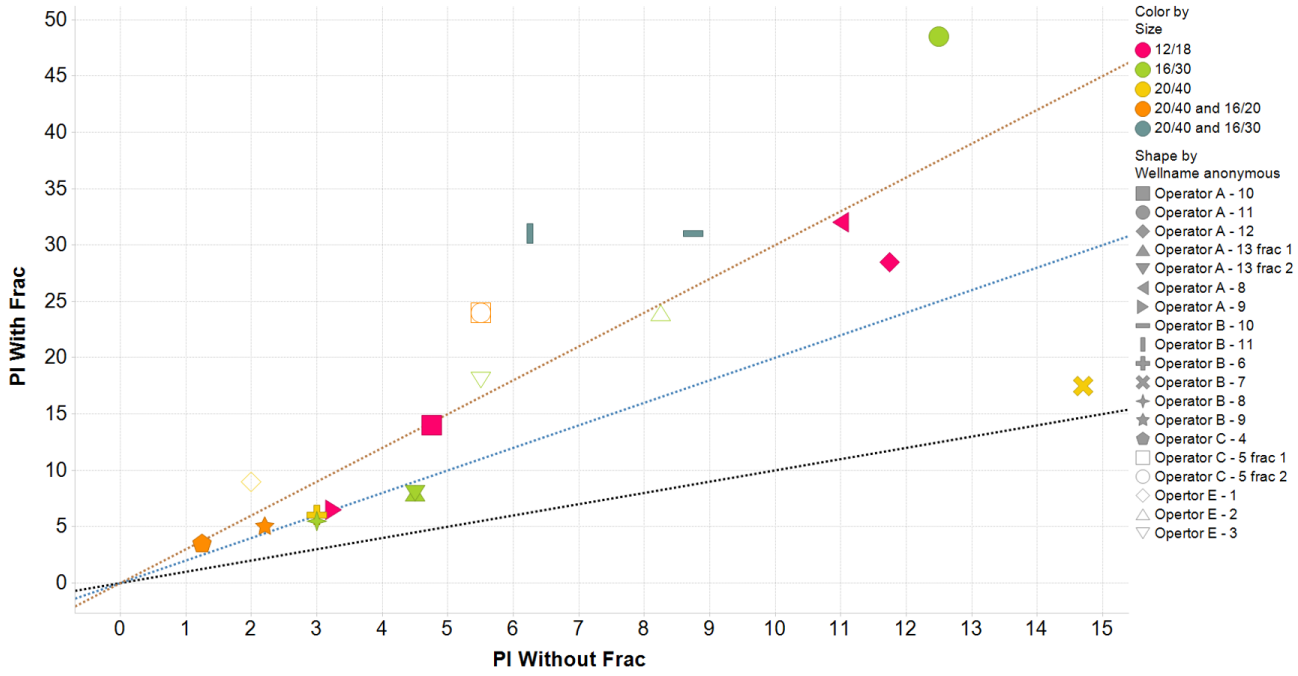


Figure 5.6: Productivity Index without (x-axis) and with fracture (y-axis) expressed in $\frac{10^3 m^3/d}{10^6 kPa^2/\mu Pas}$. The PI with fracture is determined in the FMB, while the PI without fracture is calculated with the modeled pressures and flowrates. The three lines that are drawn indicate the PI increment factor lines: the black line is no increase, the blue line is a doubling and the orange line is a tripling.

Since the wells were fractured immediately after completion, it is impossible to quantify if a fracture has connected extra dynamic GIIP. Assumed is that the dynamic GIIP determined with the fracture is equal for the model without fracture, and therefor no extra gas is connected by the fracture. The recovery factors calculated with and without a fracture, are depicted in figure 5.7. The black dashed line indicates the unchanged ultimate recovery line. The datapoints are colored to distinguish them into permeability ranges. All 19 fractures have faced a higher recovery factor after the treatment. The average recovery factor increases more than 40%: from 0.51 without fracture to 0.73 with. However, there are some outliers within the figure that requires explanation. The wells B-7, B-8 and E-1 are negative outliers. These wells are the exceptions described in section 4.4. The low increase recovery factors are caused by early exhausting of the well. Since the production did not continue until the critical rate, much lower recovery rates are observed. Furthermore, well C-4 is a positive outlier, since the productivity index has increased almost 15 times. The well is located in a tight gas field (permeability is 0.03 mD), so production without fracture is almost impossible. The predicted production rates without the fracture are on such a low rate, that it will reach critical flowrate early in production life. This is causing the low recovery rate without frac and relatively high incremental of the recovery factor. When ignoring the four outliers, the 15 wells remaining are following a certain trend. The blue dashed line is presenting this observed trend with its associated formula. Roughly taken, a hydraulic fracturing treatment ensures a recovery factor of 0.5 plus 50% of the RF before fracturing, if production continuous until critical flowrate. This recovery factor is determined on the dynamic GIIP.

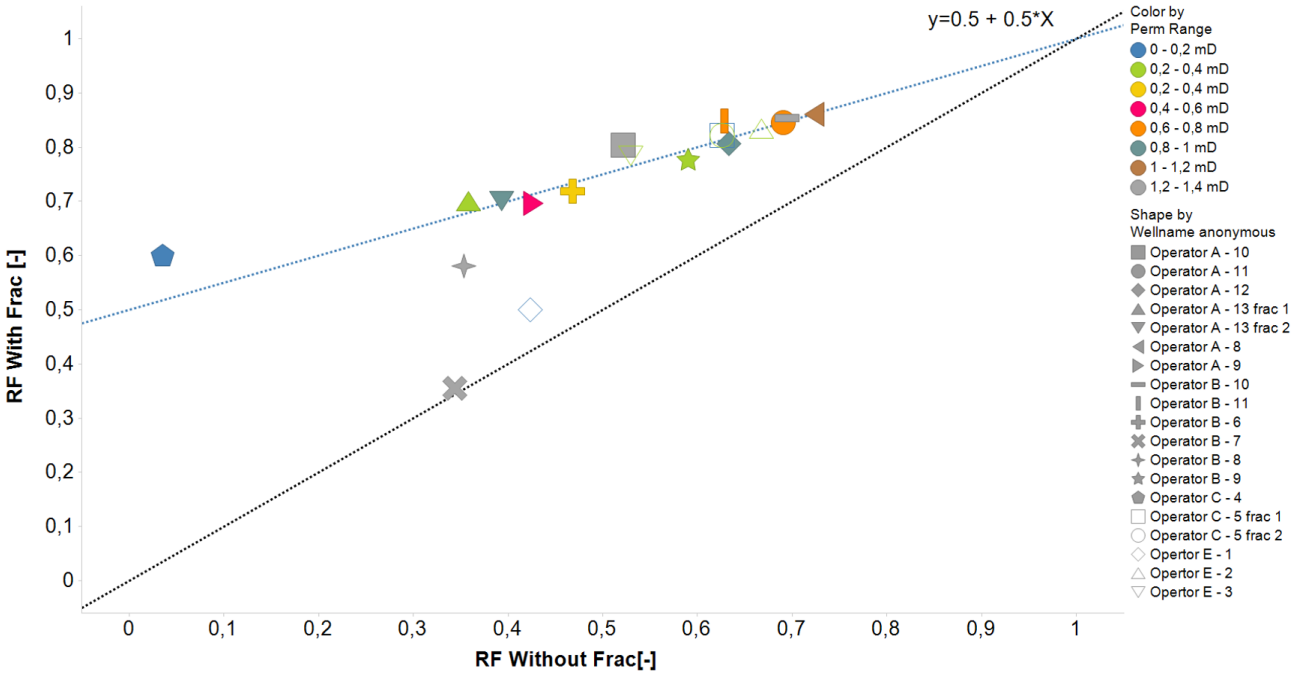


Figure 5.7: Recovery factors with and without fracture. Three negative and one positive outlier can be observed. Ignoring these outliers gives a trend indicated by the blue dashed line: a minimum RF of 0.5 plus 50% of the RF before fracturing

### 5.2.2. ECONOMICAL ANALYSIS

#### GAS INITIALLY IN PLACE

To quantify the economical value of a treatment, the net present value is also calculated for this section. The first property that immediately seems to have a relationship to a positive net present value is the dynamic gas initially in place. The link between both can be observed in figure 5.8. At the end, there is only one well having a decrease in net present value, while all other 18 fractures are gaining positive revenue. The reason for the negative NPV of well A-9 is simple: the well is connected to too little volume of gas to earn enough gas to rectify the costs of the treatment. This is also true for well C-5, which has been treated with a multiple fracture, and well E-1. These are located within the arbitrary range that has been chosen to give an indication of a transition zone between negative and positive values. Also well B-7 is located within this range, but this well is an exception caused by early exhausting.

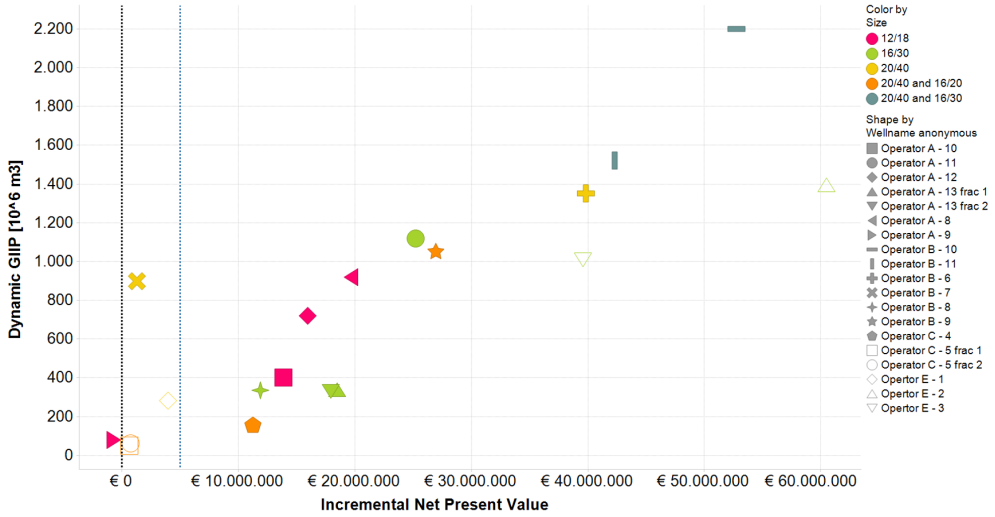


Figure 5.8: Total connected dynamic GIIP has a major influence on a positive incremental net present value. The higher the total connected GIIP, the higher the incremental NPV due to fraccing.

### FRAC PROPERTIES

Besides the volume of gas located within the reservoir, the properties of the fracture might determine the success of its treatment. The same frac properties as discussed in section 5.1.2 are important in this section. In figure 5.9 the quantity of injected proppant and the associated half length of the fracture are visible. A major difference between the wells having pre-frac data and those who are immediately fractured, is the amount of used proppant. The average quantity proppant injected in the wells having pre-frac data, is around 73,000 kg, while this is for the wells immediately fractured almost double. In these wells an average of 120,000 kg of proppant is pumped. Also the half length of the fracture (70m for with pre-frac and 90m without) and permeability (2.1 mD versus 0.6 mD) are differing enormously. Figure 5.5 indicated that the three wells treated with more than 100,000 kg of proppant were very successful fractures. In this figure the same trend can be observed. All eight wells treated with at least 100,000 kg are economically very successful. Besides this, the other trend found in the data with pre-frac data is also applicable here. The two brown dashed lines are identical to the lines in figure 5.5. If a well is treated with less than 70,000 kg of proppant and the half length of the fracture is not larger than 50 meter, the increment in added value is significantly less. One outlier to this trend is the orange dot. A plausible reason could be, that this fracture is set in one of the multiple fractured wells.

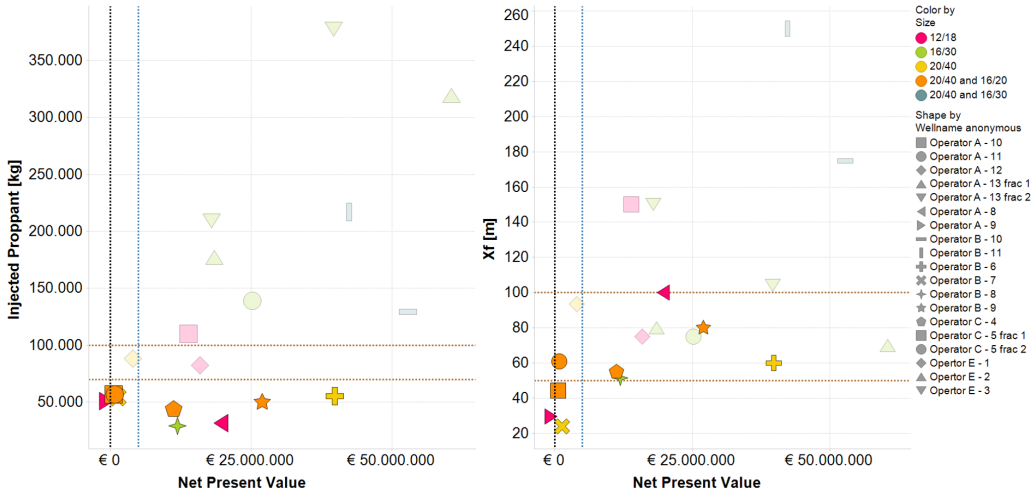


Figure 5.9: The left figure is presenting the quantity of injected proppant. The right figure is presenting the half length of the fracture. The brown dashed lines are indicating the same ranges as depicted in figure 5.5.

## 5.3. COMBINED WITH- AND WITHOUT PRE-FRAC DATA

To get a proper overview of the results together, they are summarized in this section. Within technical terms, there was only one failure out of the 38 investigated fracturing jobs, which resulted in a lower productivity index. Besides this, all treatments ensures an increment of the productivity index. The two most important properties causing higher productivity index are the matrix permeability and the half length of the fracture. In figures 5.10 and 5.11 both properties are depicted, associated with their increase in productivity index. Figure 5.10 is showing the increment of the productivity index and the associated half length fracture. The

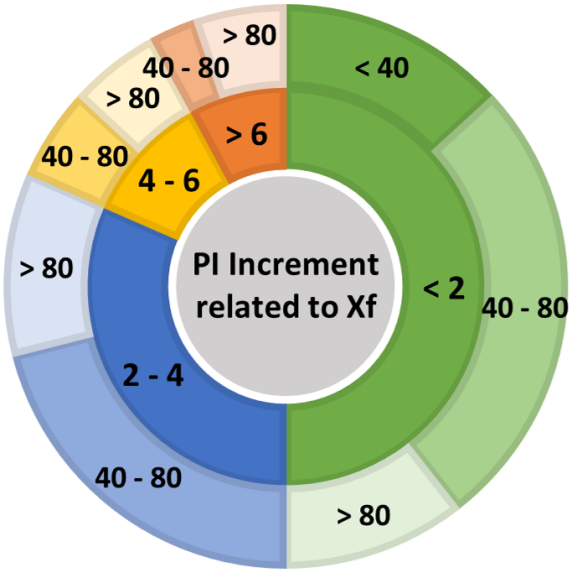


Figure 5.10: The inner ring is representing the increment in PI, classified in four different segments. The outer ring indicates the half length of the fracture, classified in three different segments

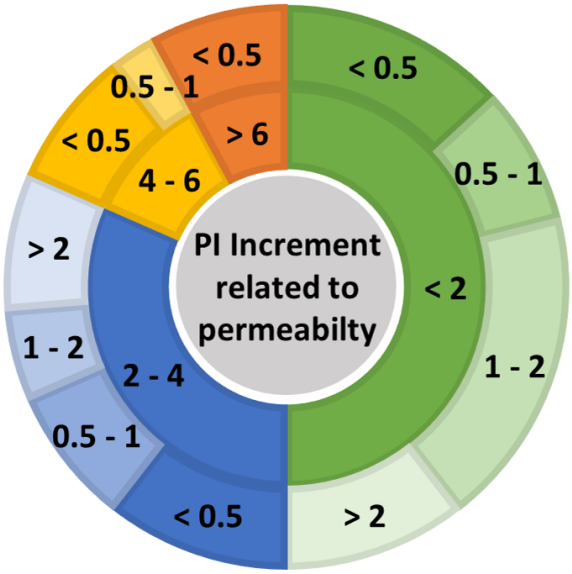


Figure 5.11: The inner ring is representing the increment in PI, classified in the identical four segments. The outer ring indicates the permeability of the matrix, classified in four different segments

inner ring is the increment in the PI and is subdivided in four different segments. The green segment indicates the PI increment less than two, the blue segment between two and four, the yellow between four and six and the red is higher than six. The outer ring is showing the half length of the fracture within the specific PI-ranges, and are subdivided into three segments: less than 40 meter, between 40 and 80 meter and greater than 80 meter. From the figure, it can be concluded that a larger fracture half length increases the chance of a higher productivity index. All wells having a half length less than 40 meter will result in a PI increment not higher than two. Fracture lengths between 40 and 80 meter are present in every segment, as well as the fracture lengths greater than 80 meter. However, the percentage of fracture lengths greater than 80 meter are increasing as the PI increment becomes higher. In the PI-increment range between two and four, almost 30% is assigned to the 80 meter fracture length. Between four-six it increases to 50%, while a PI-increase of above six is only for 67% caused by a fracture greater than 80 meter.

The permeability associated to the increase of the productivity index behaves identical and is depicted in figure 5.11. The PI-increment segments are identical to the other graph, while the outer ring is here indicating the matrix permeability. The permeability segments are subdivided into four ranges: lower than 0.5 mD, between 0.5 and 1 mD, between 1 and 2 mD and above 2 mD. In the first PI-segment, all permeability segments are present, and reservoirs having a permeability higher than 1 mD are covering more than 50%. In the second PI-segment, this percentage has already decreased to less than 50%. In the third PI-segment only reservoirs having less than 1 mD matrix permeability are present. Reservoirs having a lower permeability than 0.5 mD may cause PI increments higher than six.

All 38 hydraulic fracturing jobs have a total added value of €777 million based on the discounted cash-flows. This is an average of more than €20 million per job. There are only 3 wells having a negative value after the well has been fractured. However, the largest loss is not more than €4 million and is almost negligible compared to the total added values. The total number of treatments with different mesh proppant sizes are depicted in figure 5.12. Every color defines another proppant mesh size within the inner ring. The darkest segments within the outer ring represents the successful treatments (higher NPV than €5.000.000),

the medium bright indicates the doubtful treatments (between €0 and €5 million) and the brightest are the failures. The only segment where failures are observed, is within the 12/18 mesh size. Three out of the 12 treatments were unsuccessful. The doubtful treatments are observed within the 12/18, 20/40 and the combination of 20/40 and 16/20 mesh size segments. However, there is too little data to attribute the failures to their mesh proppant size.

The relationship between proppant size and their proceeds are summarized in figure 5.13. The inner-ring is presenting the mesh sizes while the outer-ring is the discounted cashflow (DCF). Within this outer ring the darker segments are indicating the DCF without fracture, while the brighter segments are indicating the added value of the fractures. The first thing that immediately strikes out is the 12/18 and 20/40 - 16/30 mesh sizes are covering a much bigger percentage of the graph compared to figure 5.12. It seems to be used on bigger reservoirs that were still capable of making high cashflows without fracture. The 16/30 and 20/40-16/20 segments are decreasing in size. It seems to be used on fields that are not capable of producing sufficient amounts without fracture. However, the added values in these segments are the highest with respect to the DCF without fracture. The added increment of the DCF and the added average value per well are summarized as:

- 12/18 — 26.5% increment on DCF — € 19.1 million per well
- 16/20 — 205% increment on DCF — € 22.5 million per well
- 16/30 — 61.7% increment on DCF — € 31.2 million per well
- 20/40 — 23.7% increment on DCF — € 21.8 million per well
- 20/40 and 16/20 — 130% increment on DCF — € 15.9 million per well
- 20/40 and 16/30 — 43% increment on DCF — € 48.0 million per well

However, it is not possible to draw conclusions on these numbers. There are simply too little data points to define a hard conclusion. Also, the GIIP, half length of the fracture and quantity of injected proppant are very important to the NPV, as explained earlier.

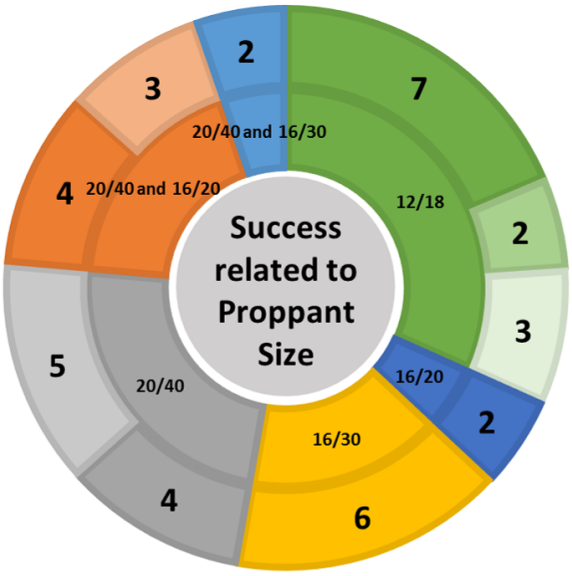


Figure 5.12: The different proppant sizes are summarized in the inner circle in different colors. The outer circle indicates the number of treatments executed. The darkest plane is showing the successful treatments, the brigther parts the doubtful ones and the brightest planes the failures (only visible in the 12/18 mesh proppant size)

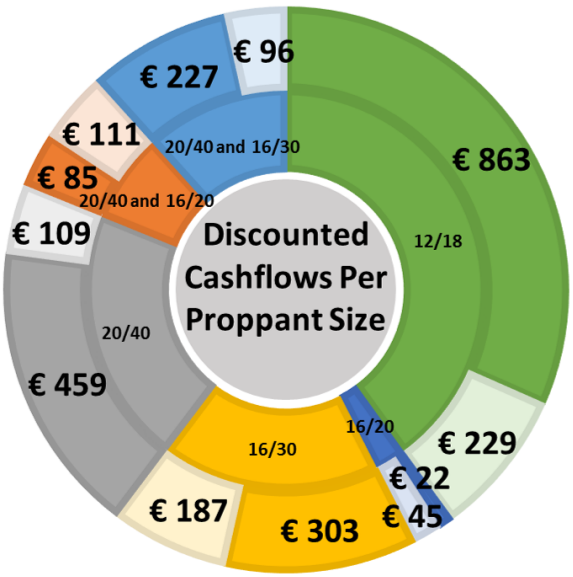


Figure 5.13: The different proppant sizes are summarized in the inner circle in different colors. The outer circle indicates the total discounted cashflow in million Euro. The darkest plane is showing the total discounted cashflow without fracture, the brighter ones are the total added value caused by fracturing

## 5.4. EXAMPLES OF TREATMENT FAILURES

Besides all decently executed hydraulic fracture treatments (37 out of 38 wells were a technical success), there are also some failures in terms of treatment performance. Two exceptions are described in this chapter to prove failures in performing a treatment are not causing immediately unrecoverable damage towards the well. Furthermore it demonstrates that the developed model with the rate transient analysis describes the forecasting quite well.

The production profile of the first failing execution is depicted in figure 5.14. The vertical dashed black line indicates the point where the fracture operation is executed. The green dots are representing the production forecast based on the history match made on the original data before the operation. These dots are overlying almost equally the original data after the operation. The cumulative production is more or less the same, indicating the production is not influenced at all by the failing treatment. During this treatment, the wireline became stuck when retrieving memory gauges after the mini fracture was conducted. Upon returning, it was impossible to set the fracture. The main fracture was aborted due to high pressures, leading to gradual decrease in injectivity. After the failed treatment, the well was cleaned-up over well test equipment. As can be seen in the figure, the production came back on the same level as it was before and the well is not further damaged by the procedure at all.

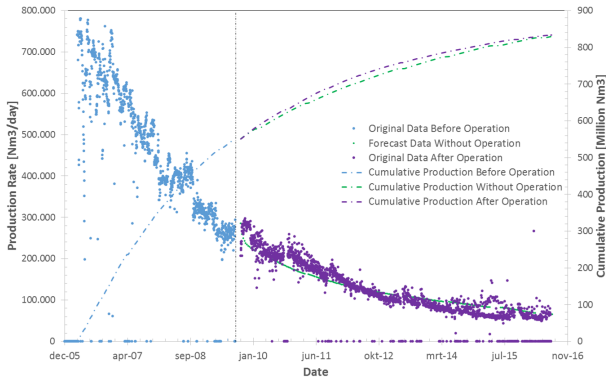


Figure 5.14: First exception. Production is on the same level as it was before the treatment. The black dashed line indicates the moment of the operation.

The second failure is depicted in figure 5.15. During the main treatment, after pumping 25% of the scheduled proppant volume, the pump failed and the mission was stopped. Upon returning, it was not possible to set the hydraulic fracture due to poor injectivity. This is most likely caused by the absence of a rathole and proppant flow-back of the first attempt. After the failed treatment, the well was cleaned-up over well test equipment. As could be seen in the figure, the production is on the same level as it was before and the well is not further damaged by the failed treatment at all.

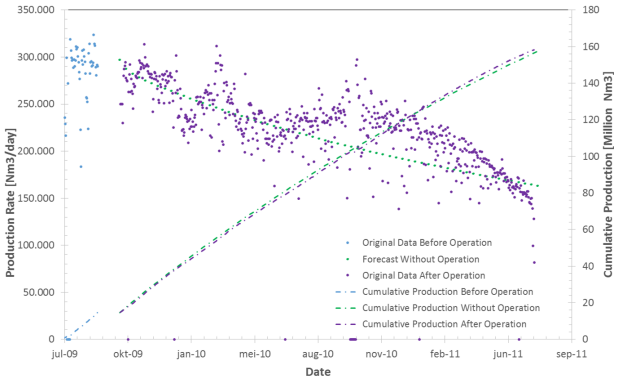


Figure 5.15: Second exception. Production is on the same level as it was before the treatment

# 6

# Discussion

During this study several limitations have been encountered that requires explanation.

## 6.1. Analytical Modeling

- The data required to perform the analyzes within this project were all taken from reports of operators. However, the gathering of the data was hard, since some operators are not willing to share this information or it is not properly stored within a database. Especially wells that are fractured a long time ago, almost no information was available. This was also one of the reasons for ignoring wells that are fractured before 1994. However, the data of recently fractured wells are mapped much better.

- The presence of other wells in the field are not taken into account. If multiple wells are located in the same block of the reservoir, it could influence the depletion of the reservoir. Especially when they are connected to the same dynamic gas volumes and communicate to each other. The inflow performance of the well will behave differently, since the reservoir pressure is depleted much faster when produced by multiple wells. This could lead to wrong determination of reservoir properties during history matching.

- The critical rate is determined by Turner and Coleman. Finally, the critical rate determined by Turner is used, since it was easier to apply to the production profiles of the wells. The huff 'n puff production behavior was observed before critical rate determined with Coleman was reached, and therefore Turner is chosen. However, the examination of Turner et al.'s published data indicates that most of the wells used in the comparison had wellhead flowing pressures above 500 psi, which is more or less 34 bar. Because gas well load up problems generally worsen with continued decline in reservoir energy, Coleman focused on wells with lower reservoir pressures that are experiencing liquid load-up and have FWHP's below 500 psi[24]. Since this project is focusing on a critical rate with FWHP of 15 bar, it is probably more accurate to use the Coleman rate instead of Turner's.

## 6.2. Economic Analysis

- The downtime of a well is not properly taken into account. Although the downtime has been implemented in forecasting procedures, there is still a difference between wells. Some wells are having enormous downtimes (up to 40%) while others are producing almost continuously (less than 5% downtime). This will have an impact on the net present value of a treatment. If there is less downtime, the NPV will automatically become higher. However, a trend between downtime and NPV has not been observed, as indicated in figure C.11 in Appendix C.3. Also the production duration is not taken into account. A well with a longer production duration will have a higher NPV compared to a short one, when hydraulic fracturing is properly applied. In figure 6.1 an overview of the percentage and days of downtime is given. The graph is divided into ranges indicating the percentage of downtime. The blue colored bar indicates the wells that have less than 500 days downtime, the green between 500 and 1000 days and the gray more than 1000 days downtime.

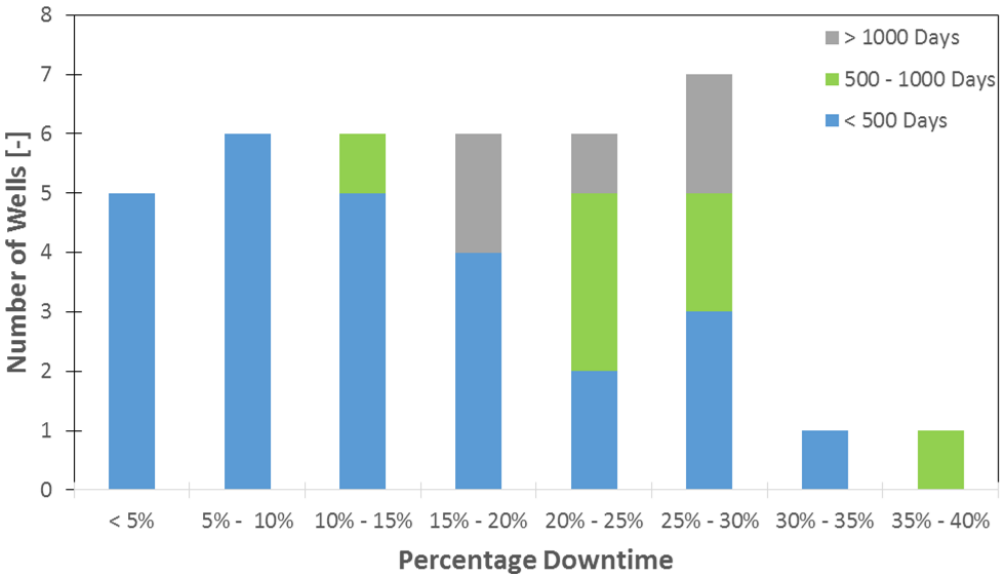


Figure 6.1: Percentage downtime divided in eight ranges. A blue bar indicates less than 500 days of downtime, green is downtime between 500 and 1000 days, gray indicates downtime of more than 1000 days.

- For a randomly chosen well, a tornado plot is constructed to show the sensitivity towards the NPV. This tornado plot can be seen in figure C.12 in Appendix C.3. Only four parameters are discussed: discountrate, AFE, gasprice and the caloric value of the gas. Although reservoir properties such as matrix permeability or GIIP could also be conducted to a sensitivity analysis, this will lead to an inconsistent history match. All the four values are taken 20% higher and 20% lower than its original value. It can be seen that a change in caloric value and gas price are most sensitive towards the NPV.
- The FWHP of 15 bar which is used for forecasting as discussed in figure 3.4, has the highest productivity at the beginning of production. However, producing from the beginning with 15 bar FWHP is not very realistic, since compression is needed. Compression equipment will come with a price, which is offshore normally quite expensive. Therefor successive decreasing the FWHP from 100 to 15 bar is more realistic. However, this was not applicable to all wells investigated since some wells were producing below 50 bar already and therefore 15 bar FWHP was chosen as forecasting pressure. Although it worked out quite well, it leads sometimes in a too optimistic discounted cashflows. An example is given in figure 6.2. In figure 6.2(a) the production profile of both the FWHP procedures is given, and in figure 6.2(b) its effect on the discounted cashflows can be seen. The difference between both is €13 million (almost 10% of the total DCF in this case), and is gained immediately in the first year, since the production in the beginning with 15 bar FWHP is much higher. Although the cumulative production is equally at the end of forecasting, the difference of DCF is considerably.

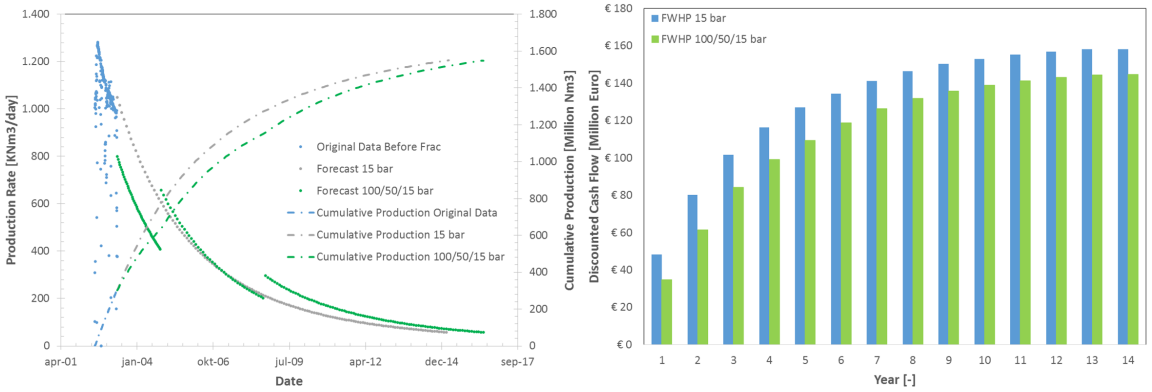


(a) Forecast with two different approaches: constant FWHP of 15 bar and successive decrease from 100, to 50 and finally 15 bar.

(b) The influence of the two different approaches on discounted cashflow.

Figure 6.2: Production profile and its effect on DCF

## 6.3. ACCURACY ANALYSIS

- The analytical model without fracture which is built on the wells that were immediately hydraulic fractured, are all modeled with a skin of 0. However, this is probably an underestimation, since a potential candidate well for hydraulic fracture treatment has normally a high skin factor. Therefor skin factors of 2.5, 5 and 10 are modeled for a randomly chosen well to show the effect on production. This can be seen in figure 6.3. The cumulative production decreases significantly if the skin factor increases. There is almost 300 million N$m^3$ less production when the well has a skin factor of 10. Also the productivity decreases enormously, especially in early times production. The initial flowrate is more or less halved, from 370 KN$m^3$/day with 0 skin to 180 KN$m^3$/day with skin factor of 10. This productivity decrease in early times has a major impact on the discounted cash flow. In this particular case, the DCF decreases from € 95 million with 0 skin, to € 60 million with skin factor of 10.

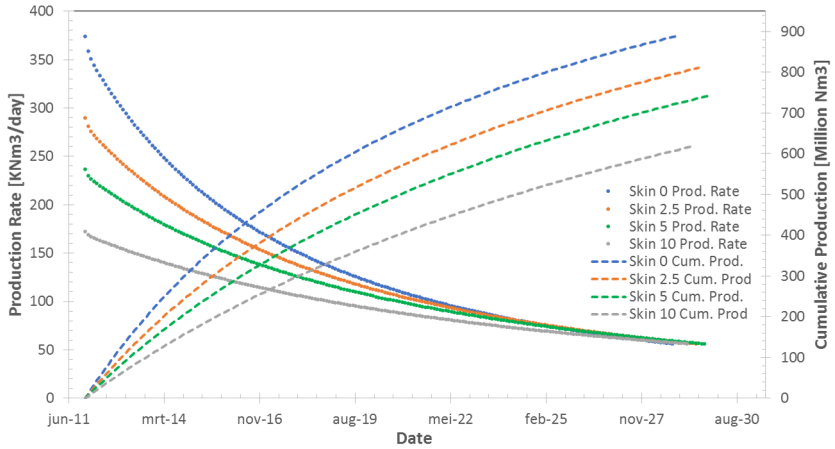


Figure 6.3: The influence of a higher skin factor on the production rates. This behavior is applicable to the analytical models without fracture build on the wells that were immediately fractured. Skin factors are ranging from 0 (blue), 2.5 (orange), 5 (green) to 10 (gray)

- The decline curves are used to get an indication of the dynamic GIIP and for a quality control of the forecast generated by RTA. In figure 6.4 the quality control is given. The range between zero and one indicates the range of predicted cumulative production by decline curves. At zero, the exponential decline is located, while harmonic decline is at one. The blue dots within this range are the predicted volumes generated by RTA. Almost all wells are located within this range, except the red dots. These are

indicating the cumulative production determined with RTA who are less than production determined by DCA. However, those four wells are presenting outliers: the exhausted wells that are not producing to the critical flowrate. Only 29 wells are visible within the figure, since for nine wells it was not possible to construct a proper decline curve, due to noisy data.

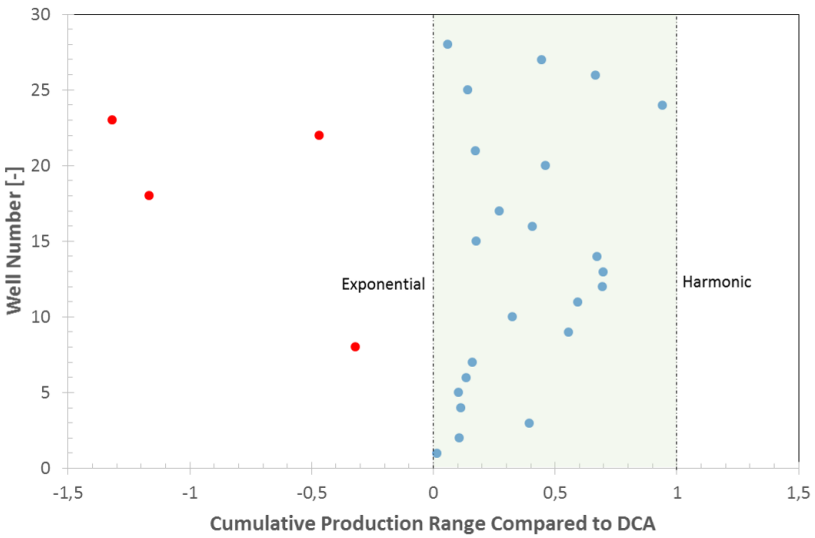


Figure 6.4: The forecasts generated by RTA compared to DCA.

- The biggest uncertainty within this project is the size of the dataset. There are 38 successful hydraulic fractures investigated, which is almost 12% of all fracturing treatments in The Netherlands. The reason for this quantity is already discussed in section 1. The conclusions drawn within this report become more valuable when more hydraulic fracturing treatments can be investigated and are showing the same behavior. Since the dataset was not big enough, probability functions such as normal distribution did not work out properly. The spread within the measured properties and parameters was too big to handle with the size of the dataset.

## 6.4. COMPARISON WITH LITERATURE

Although rate transient analysis is a reliable method to model production behavior, it is not commonly used in the industry. Almost all forecasting models are still based on decline curve analysis. However, in the literature some research can be found that is done via RTA. Santacruz et al performed a study with more than 325 wells in the Haynesville Shale. All wells are evaluated by RTA since making forecasts with the overpressured reservoir was challenging using DCA. Since the production data was coming from shale reservoirs, all history matches are made with the horizontal multifrac model. This resulted in a reliable forecasting methodology and correlations were found and confirmed by geological modeling and reservoir surveillance[30]. However, the project is not comparable to this project since horizontal wells in shale reservoirs behaves differently from the vertical wells in this project.

A similar study was performed by Joo et al. on a tight gas field which was produced by a horizontal well which was fractured multiple times. However, they assumed time depending changes in stimulated reservoir volumes (SRV), while in this project the dynamic GIIP is a fixed value over time, unless the fracturing treatment connects extra dynamic gas[31]. The SRV is an emperical replacement fore reliable modeling used in shale gas reservoirs, since the fracture planes are generated more complex compared to sandstone fractures. The multistage fracture treatments often overlap and interact in intricate ways with natural fractures in the rock[32]. Similar studies on shale gas reservoir with RTA techniques are performed by Wei et al. and Duong[33][34].

Murminacho et al. conducted a research to production and reserves increment in a mature oil field which is hydraulically fractured. This was done by combining three types of analyzes: fracture pressure, pressure transient and rate transient. The production increased on average 300 BOPD per fractured well. The reservoir parameters determined by the three types were shown to provide reliable and similar values for transmissibil-

ity and pressure in the formation. Furthermore a remarkable increase in the reserves by DCA was identified after hydraulic fracturing (up to more than 10 times in some cases)[35]. Another research to hydraulic fracturing in an oil field is done by Clarkson et al. They performed a field case to a multi fractured horizontal well completed in a low-permeability area of the Pembina Cardium Field in Canada. They concluded that the analytical approach for history matching and forecasting tight oil reservoirs appears to work well for a wide range of reservoir and hydraulic fracture properties[36].

# 7

# CONCLUSION

The following conclusions have been drawn from this study based on the 38 investigated fracturing treatments:

1. General
    - Hydraulic fracturing increases the productivity in almost all wells: 37 out of the 38 investigated wells had an increment in the productivity index. There was only one well having a lower PI after the treatment. However this well was fractured too late in production life to have a sufficient impact. On average, the productivity index has been increased by a factor 2.8 after the well was fractured. The two most important properties creating the PI increment are a low matrix permeability and a large half length of the fracture.
    - The frac properties might determine the success of a treatment. The two properties found to be the most important are quantity of injected proppant and fracture half length. It was observed that an amount higher than 100,000 kg of pumped proppant lead to a high economic gain. If the amount of injected proppant is lower than 70,000 kg and the half length of the fracture is equal to or lower than 50 meter, the fracturing results in a net present value lower than € 5,000,000.
    - Three out of the 38 investigated wells were an economic failure. All these wells are treated with the 12/18 mesh size.
    - An average discounted added value of € 20 million per job is created by hydraulic fracturing.
    - Two examples of treatment failures showed there was no unrecoverable damage towards the well. Same production levels were reached after clean-up.
    - Other reservoir- or frac properties seem not to correlate with the NPV.
2. Wells with pre-frac data
    - The timing of a hydraulic fracturing treatment is considered to be an important aspect associated with economic success. The earlier a treatment is conducted within its production life, the bigger chance of gaining high economic values. It seems that wells that have been fractured before the reservoir pressure is depleted by 35% are an economic success. The combination of high remaining pressures and large remaining gas volumes are the main reasons.
    - Wells that are stimulated later in production life (after 35% of reservoir pressure is depleted) are only gaining large economic value, if they connect extra dynamic GIIP to the well or increase their productivity enormously.
3. Wells without pre-frac data
    - A trend is observed in the increase of the recovery factory. Roughly taken, a hydraulic fracturing treatment ensures a recovery factor of 0.5, plus 50% of the RF before fracturing.
    - Total connected dynamic GIIP has a major influence on a positive incremental net present value. The higher the total dynamic connected GIIP, the higher the incremental NPV due to fracturing treatments.

# 8

# RECOMMENDATIONS

The conclusion of the thesis is that all objectives have been met and that very interesting relationships have been discovered. The thesis reveals a robust insight into the technical and commercial effects of hydraulic fracturing. Though follow up analysis would further underpin the main findings, the current work can be applied to optimize the timing and methods of hydraulic fracturing of gas reservoirs. This will undoubtedly facilitate the achievement of the most beneficial commercial results. Some suggestions for further research could be the following:

*Liquid Gas Ratio*
An important issue that could make the model much more precise, is the implementation of water and condensate production. Perhaps IHS Harmony is able to handle the huff 'n puff production behavior when the liquid production is taken into account. Also the cut-off criterion based on the Turner rate could be ignored in that situation. However, the reason for not implementing the liquid production in this study, it was not recorded or stored properly by the operators.

*Horizontal Wells*
Three horizontal multi fractured wells are modeled in this study by RTA in IHS Harmony. However, the outcome was not comparable to the vertical fractured wells, and therefor not taken into account in this project. Although they are not comparable, a horizontal multi fractured model could be made based on more horizontal wells. This should be possible, since there are at least 15 horizontal wells fractured in The Netherlands. This could also be done for oil wells.

*Simulation Model*
It is recommended to verify the model with future production rates. Hereby the predicted flow rates can be compared with real data to validate the model and gain more insights.

*Data*
For this project the data used is all coming from The Netherlands. Including data from other fractured wells, and therefor creating a bigger dataset, could increase the quality of the project enormously. Since only 38 out of 338 fracturing treatments are investigated in this project, there is still a lot of research to do. However, the reason for not including these wells in this project was the lack of qualitative data. Also data analysis from other countries could be included. Especially in the USA a lot of wells are hydraulically fractured (normally multiple times) to unlock the potential of shale reservoirs. But also in neighboring countries such as the United Kingdom, fraccing is not unusual: over 200 wells are stimulated onshore by hydraulic fracturing in the UK [37].

# A

# APPENDIX-A

The principle of all gas compressibility factors is the law of corresponding states and is developed by Van Der Waals. The law proposes that all gases will exhibit the same behavior, expressed in the Z-Factor. Two correlations used in this study are the Beggs- and Brill correlation and the Benedict Webb Rubin correlation. The Z-factor is in both correlations defined as in equation (A).

$$Z = f(T_r, P_r) \tag{A.1}$$

### A.0.1. BEGGS- AND BRILL CORRELATION

$$Z = A + (1 - A)exp(-B) + CP_{pr}^{D} \tag{A.2}$$

where

$$A = 1.39(T_{pr} - 0.92)^{0.5} - 0.36T_{pr} - 0.101 \tag{A.3}$$

$$B = \left(0.62 - 0.23T_{pr}\right)P_{pr} + \left(\frac{0.066}{T_{pr} - 0.86} - 0.037\right)P_{pr}^{2} + \left(\frac{0.32}{10^{(9(T_{pr}-1))}}\right)P_{pr}^{6} \tag{A.4}$$

$$C = 0.132 - 0.32log(T_{pr}) \tag{A.5}$$

$$D = 10^{0.3106 - 0.49T_{pr} + 0.1824T_{pr}^{2}} \tag{A.6}$$

The critical pressures and temperatures are by definition,

$$T_r = \frac{T}{T_c} \tag{A.7}$$

$$p_r = \frac{p}{p_c} \tag{A.8}$$

The gas composition is influencing the critical pressure and temperature.

$$T_c = \sum_i x_i T_{c,i} \tag{A.9}$$

$$p_c = \sum_i x_i p_{c,i} \tag{A.10}$$

### A.0.2. BENEDICT-WEBB-RUBIN CORRELATION

$$Z = 1 + \left(A_1 + \frac{A_2}{T_r} + \frac{A_2}{T_r^3}\right)\rho_r + \left(A_4 + \frac{A_5}{T_r}\right)\rho_r^2 + A_5A_6\frac{\rho_r^5}{T_r} + A_7\frac{\rho_r^2}{T_r^3} + (1 + A_8\rho_r^2)e^{-1+A_8\rho_r^2} \tag{A.11}$$

where

$A_1$ = 0.31506237 $A_2$ = -1.04670990 $A_3$ = -0.57832729 $A_4$ = 0.53530771

$A_5$ = -0.61232032 $A_6$ = -0.10488813 $A_7$ = 0.68157001 $A_8$ = 0.68446549

The critical pressures and temperatures are calculated differently compared with the Beggs- and Brill equation. The original $T_c$ and $P_c$ are calculated via equation(A.9) and (A.10), but there is an extra correction term for sour gas. This extra correction term is presented in equation(A.12).

$$\epsilon_3 = 120(A^{0.9} - A^{1.6}) + 15(B^{0.5} - B^{0.4}) \tag{A.12}$$

This $\epsilon_3$ will be inserted to equation (A.13) and (A.14), leading to different reduced temperatures and pressures (A.15)(A.16).

$$T_c' = T_c - \epsilon_3 \tag{A.13}$$

$$p_c' = \frac{p_c T_c}{T_c + B(1-B)\epsilon_3} \tag{A.14}$$

$$T_r = \frac{T}{T_c'} \tag{A.15}$$

$$p_r = \frac{p}{p_c'} \tag{A.16}$$

Based on the corrected reduced pressure and temperature, the $\rho_r$ can be calculated as

$$\rho_r = 0.27\frac{p_r}{ZT_r} \tag{A.17}$$

To define the critical flowrate at the surface, the ideal gas law is used.

$$pV = nRTZ \tag{A.18}$$

where:

| | | |
|---|---|---|
| P | = | Pressure $[Pa]$ |
| V | = | Volume $[m^3]$ |
| n | = | Number of Moles $[-]$ |
| R | = | Gas Constant $[JK^{-1}mol^{-1}]$ |
| T | = | Temperature $[K]$ |

Assumed is the mole amount is equally in the reservoir as it is on the surface. For both cases the ideal gas law could be written as equation(A.19) and (A.20)

$$p_{sc}V_{sc} = nRT_{sc} \tag{A.19}$$

$$pV = nRTZ \tag{A.20}$$

Make it in both cases a function of $n$ and set them equally gives equation(A.21)

$$V_{sc} = \frac{pVT_{sc}}{p_{sc}TZ} \tag{A.21}$$

Put it in time perspective and V is equal to the calculated critical velocity times the area gives the final critical flowrate formula in equation(A.22)

$$Q_{crit} = \frac{pu_{crit}AT_{sc}}{p_{sc}TZ} \tag{A.22}$$

### A.0.3. MATERIAL BALANCE

The FMB is built on the ideal gas law as presented in equations A.18, A.19 and A.20. Putting this equations together in the expansion factor formula from equation 3.5 gives the following equation A.23

$$E = \frac{T_{sc}}{P_{sc}T} \times \frac{P}{Z} = \alpha\frac{P}{Z} \tag{A.23}$$

Modification of equation 3.4 via the following derivation and filling in equation A.23 will give the p/Z function for the static material balance as explained in equation 3.6

$$\frac{G_i}{E_i} = \frac{1}{E}\left(G_i - G_p\right) \tag{A.24}$$

Dividing by $G_i$

$$\frac{1}{E_i} = \frac{1}{E}\left(1 - \frac{G_p}{G}\right) \tag{A.25}$$

Rearranging the formula

$$E = E_i\left(1 - \frac{G_p}{G}\right) \tag{A.26}$$

Filling in equation A.23 gives

$$\alpha\frac{P}{Z} = \alpha\frac{P_i}{Z_i}\left(1 - \frac{G_p}{G}\right) \tag{A.27}$$

$\alpha$ cancels out and results in the final static material balance equation as presented in equation 3.6

# B

# APPENDIX-B

| Sieve Mesh Size | Equivalent Particle Diameter (mm) | Nominal Particle Diameter (mm) | Weight % Retained | | |
|---|---|---|---|---|---|
| | | | Extended PSD-3 | Comp. Ex. A | Comp. Ex. B |
| 16 | >1.18 mm | ~1.6 | 0.5 | 0.0 | 0.0 |
| 18 | 1.0-1.18 mm | 1.09 | 5.6 | 0.0 | 0.0 |
| 20 | 0.85-1.0 mm | 0.93 | 24.5 | 3.7 | 5.0 |
| 25 | 0.71-0.85 mm | 0.78 | 24.1 | 28.6 | 33.0 |
| 30 | 0.60-0.71 mm | 0.66 | 23.2 | 31.4 | 35.0 |
| 35 | 0.50-0.60 mm | 0.55 | 14.4 | 34.3 | 20.0 |
| 40 | 0.425-0.50 mm | 0.46 | 7.1 | 2.0 | 6.0 |
| 45 | 0.355-0.425 mm | 0.39 | 0.5 | 0.0 | 1.0 |
| 50 | 0.30-0.355 mm | 0.33 | 0.1 | 0.0 | 0.0 |

Figure B.1: The sizes of the proppant

# C

# APPENDIX-C

## C.1. WITH PRE-FRAC DATA

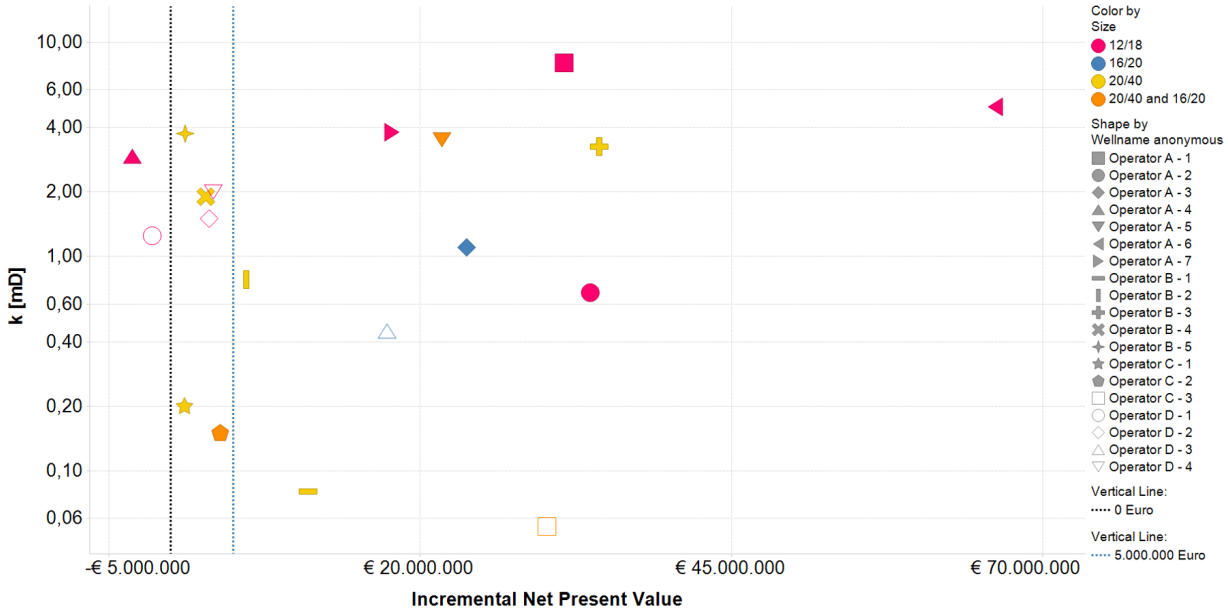


Figure C.1: Permeability as function of the increment in net present value for wells that have pre-frac data. The permeabilities are much higher compared to the wells that are fracced immediately, as can be seen in figure C.6.

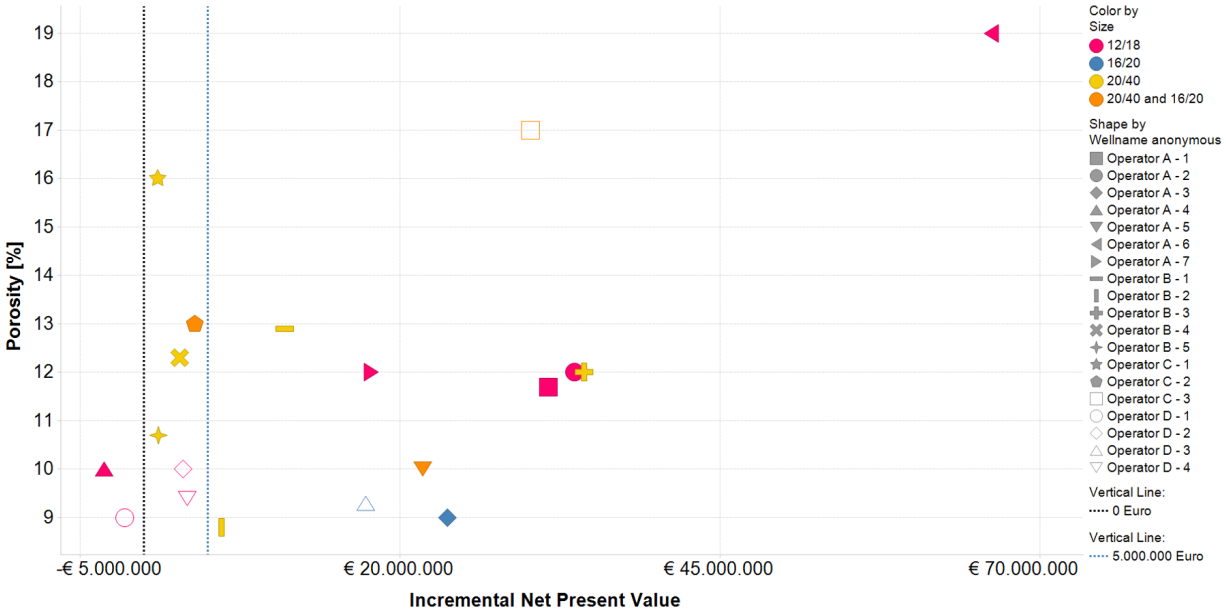


Figure C.2: Porosity as function of the increment in net present value for wells that have pre-frac data.

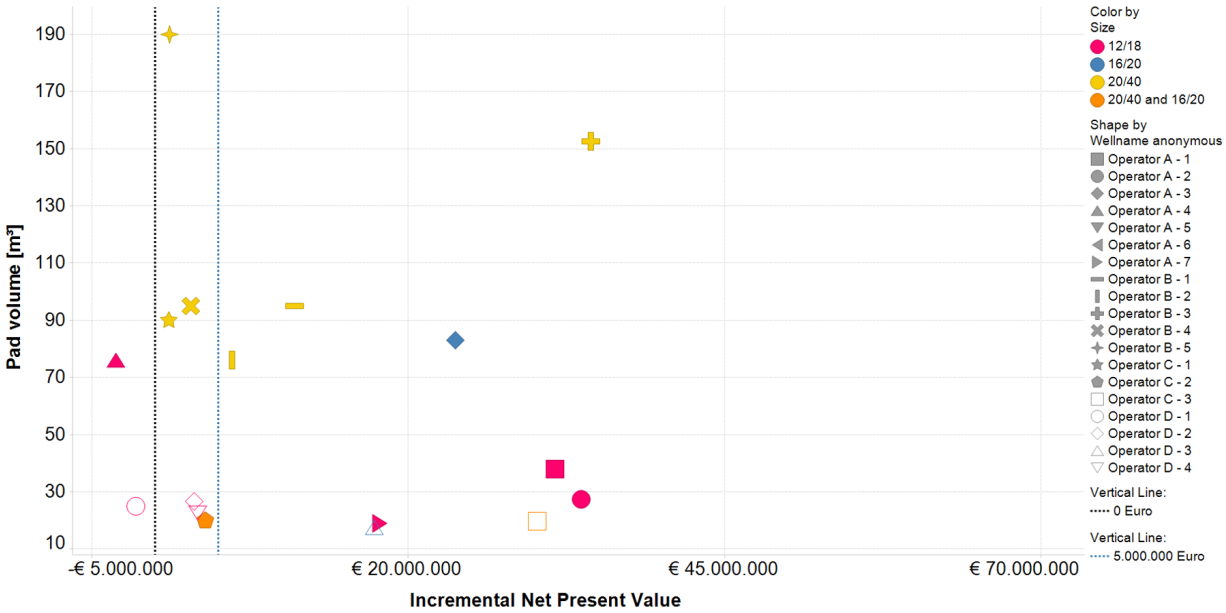


Figure C.3: Pad volume pumped as function of the increment in NPV. Not all the wells are visible within the graph since it was not possible to collect all Pad volumes pumped.

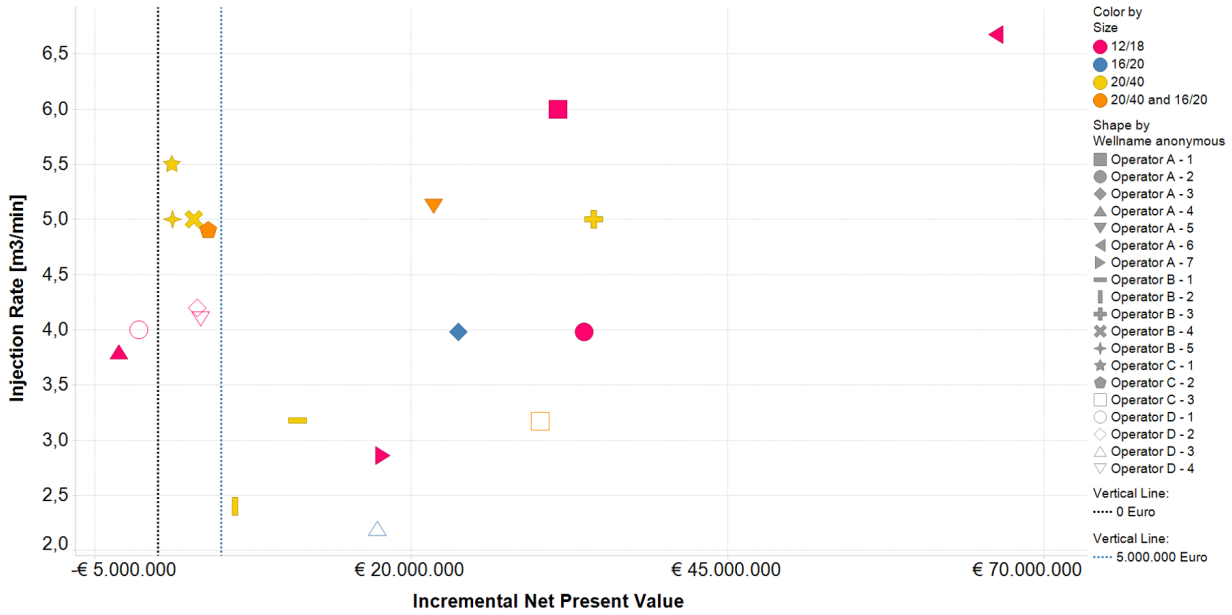


Figure C.4: The injection rate per well as function of the increment in NPV. The injection rate is actually only depending on the power of the pump. More power means higher pumping rate.

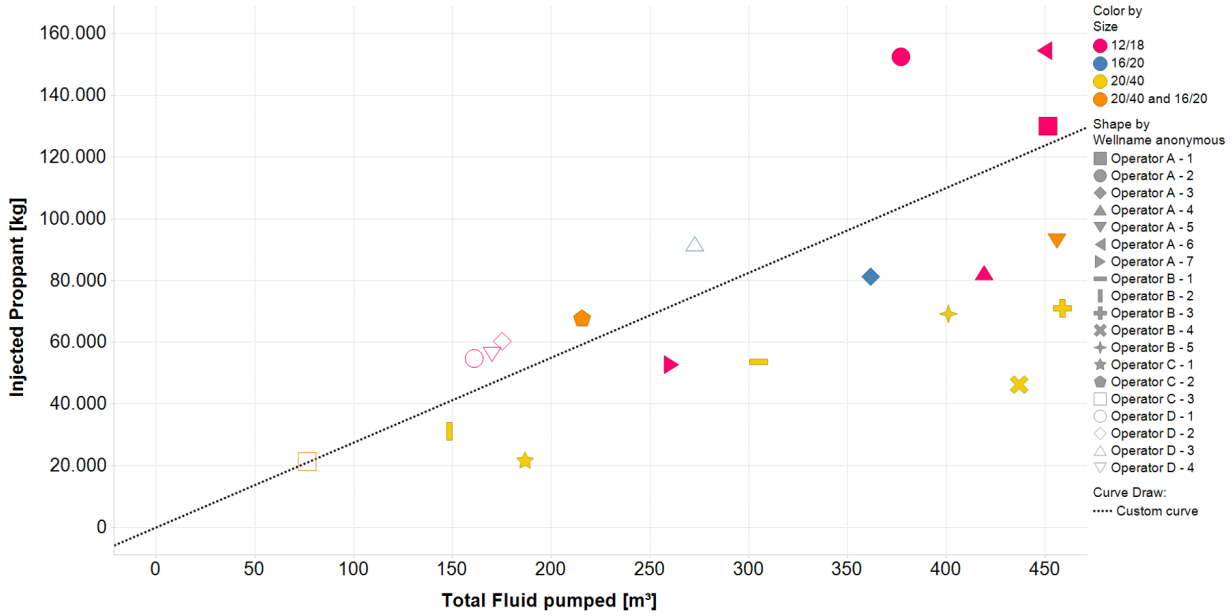


Figure C.5: The concentration of proppant in the pumped fluid. The black dashed line is roughly indicating the average concentration: 275 kg proppant per $m^3$ fluid.

## C.2. WITHOUT PRE-FRAC DATA

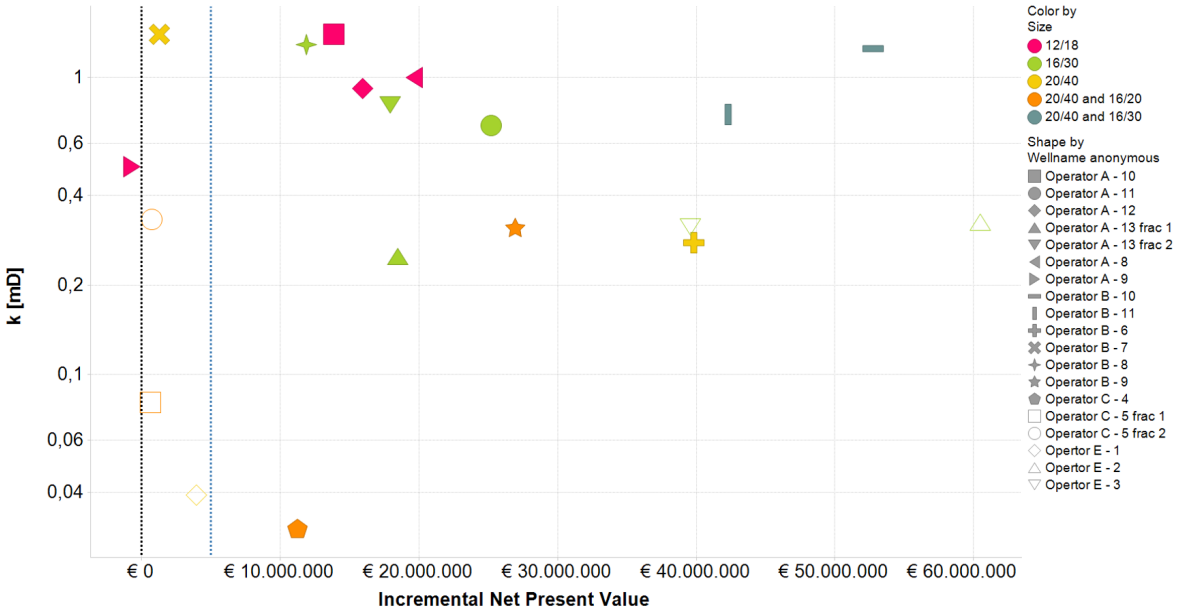


Figure C.6: Permeability as function of the increment in net present value for wells that do not have pre-frac data. The permeabilities are much lower compared to the wells that are fracced later in production life

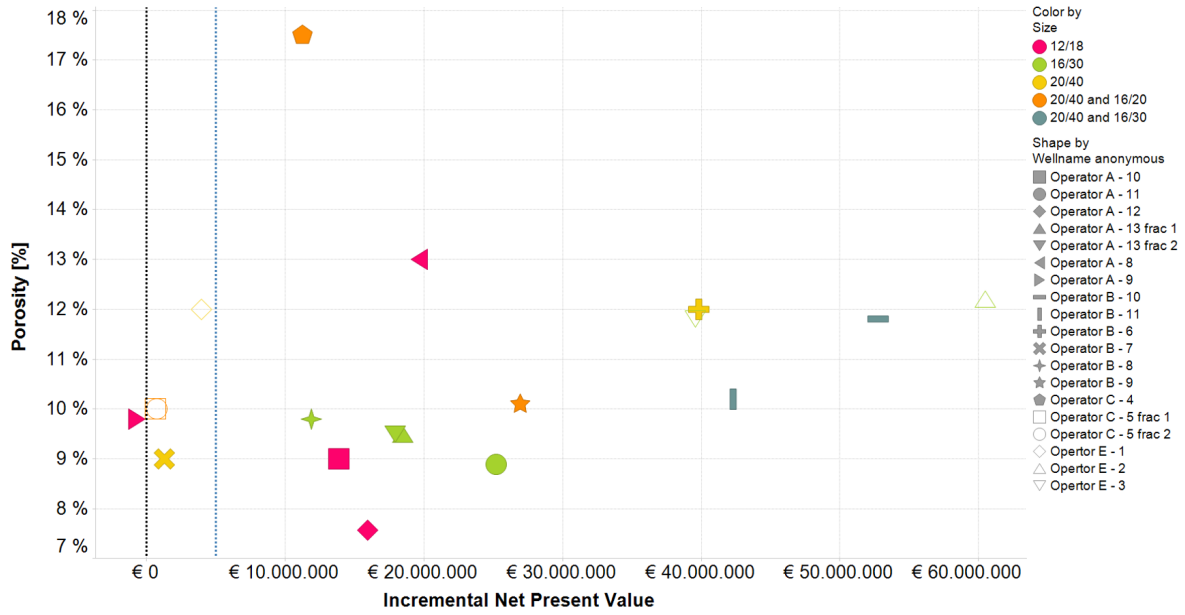


Figure C.7: Porosity as function of the increment in net present value for wells that do not have pre-frac data.

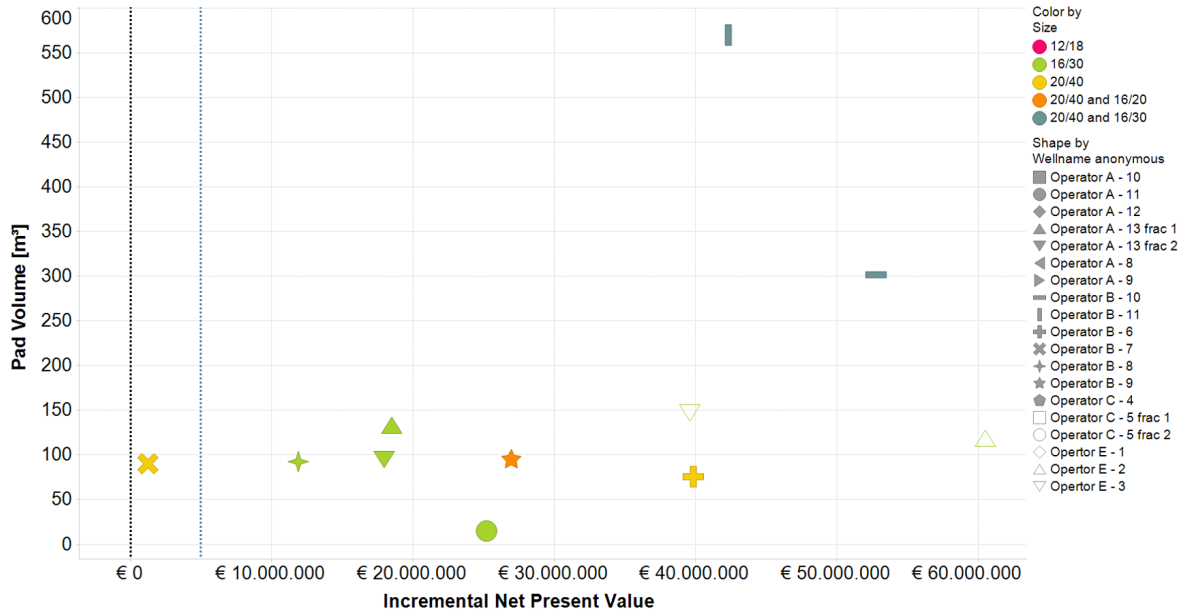


Figure C.8: Pad volume pumped as function of the increment in NPV. Not all the wells are visible within the graph since it was not possible to collect all Pad volumes pumped. It can be observed that injected pad volumes are much higher compared to the wells that are fractured later in production life.

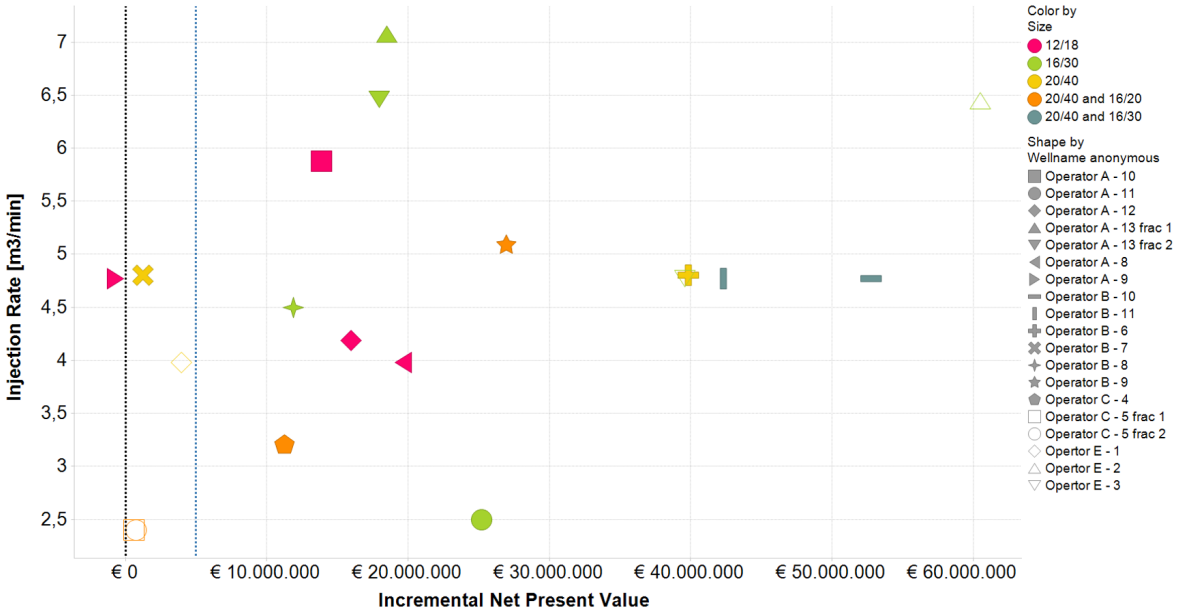


Figure C.9: The injection rate per well as function of the increment in NPV. The injection rate is actually only depending on the power of the pump. More power means higher pumping rate.

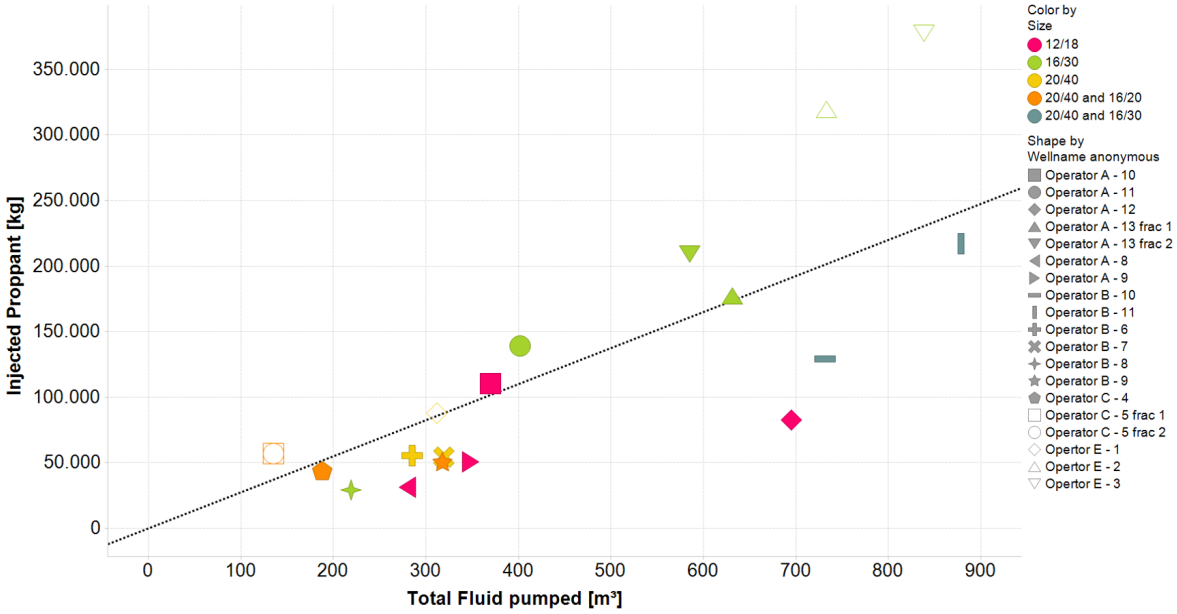


Figure C.10: The concentration of proppant in the pumped fluid. The black dashed line is roughly indicating the average concentration and is almost equally to figure C.5: 275 kg proppant per $m^3$ fluid. Since the amount of pumped proppant is much higher compared to the wells that are fractured later in production life, the total fluid pumped is also much higher.

## C.3. GENERAL

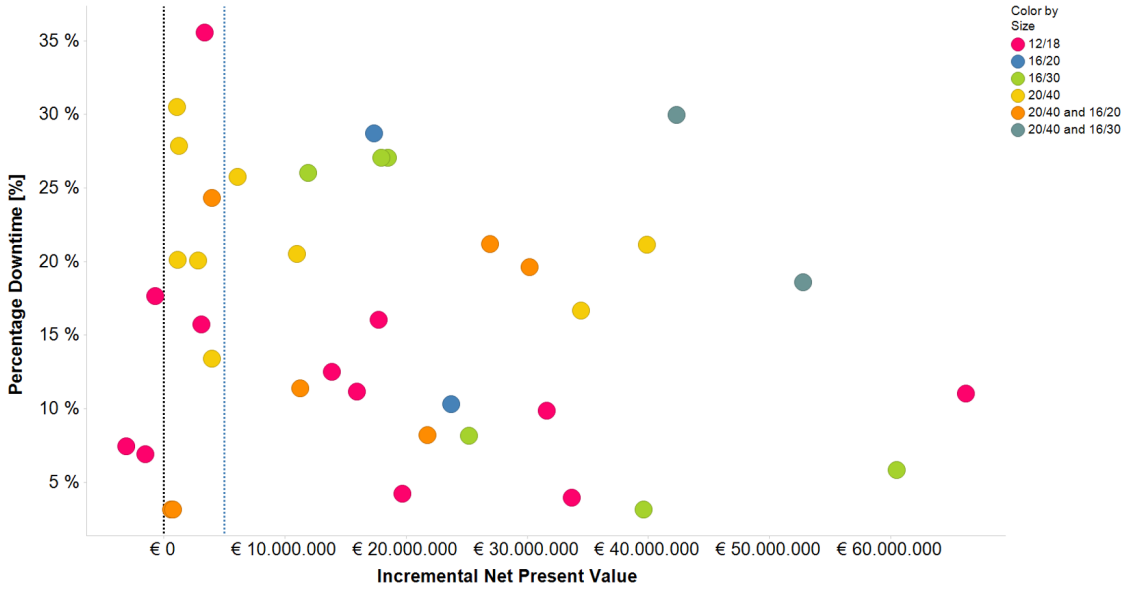


Figure C.11: Percentage of downtime as function of the increment in NPV. All data point are scattered such that there is no proof high downtimes lead to low economic values.

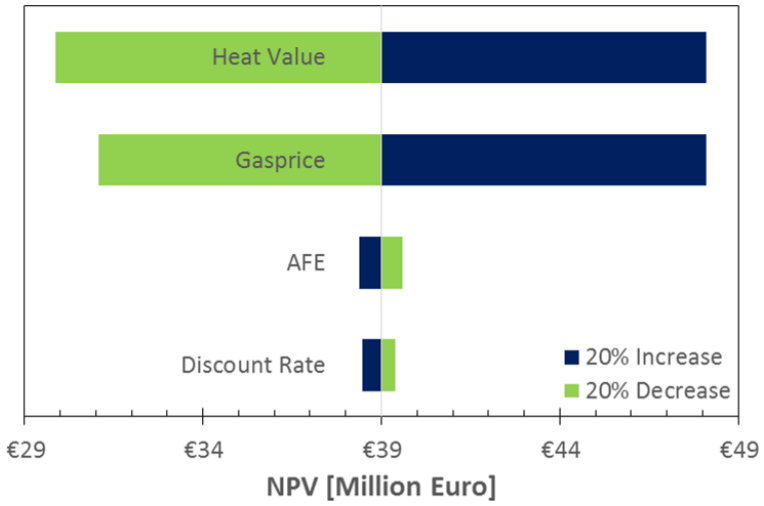


Figure C.12: Tornado plot for economic analysis. Only heat value, gasprice, AFE and the discount rate are taken into account. Although reservoir properties such as GIIP or permeability could also be conducted to a sensitivity analysis, this will lead to an inconsistent history match. Therefore they are not used in this sensitivity study. The heat value, which depends on the caloric value of the gas, and the gas price are the properties most sensitive to a change in NPV.

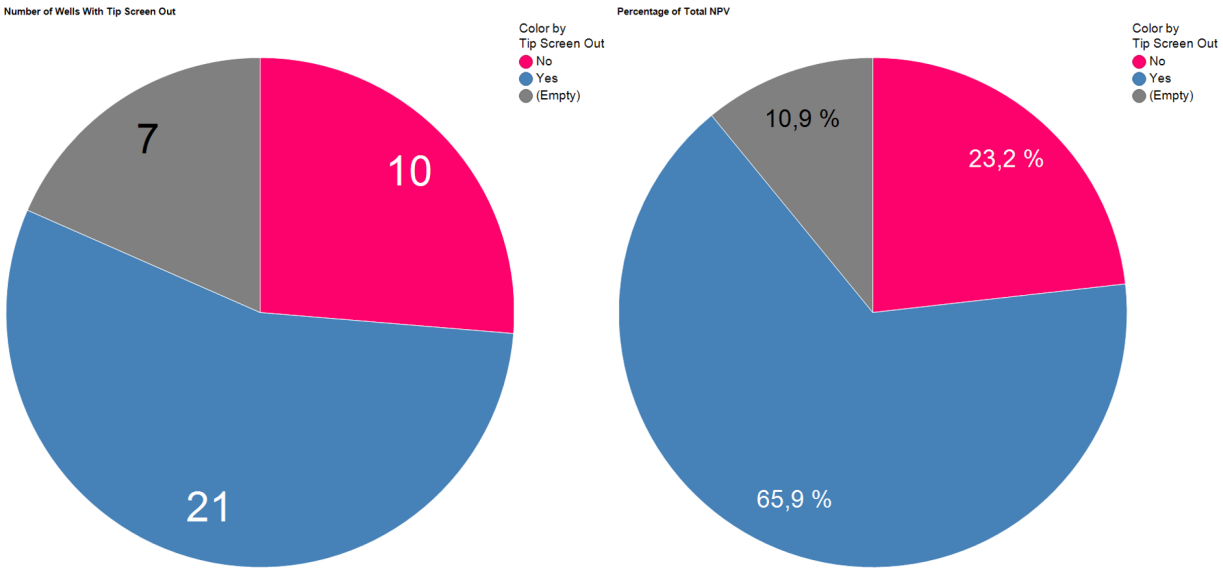


Figure C.13: Tip Screen Out procedures used during fracturing per well. The blue parts are indicating the well was fractured with a TSO procedure. The pink are fractured with the regular fracturing method and the black parts are unknown, since it was not found in the reports. The left figure represents the number of wells, the right figure the percentage of the NPV caused by the different treatments.

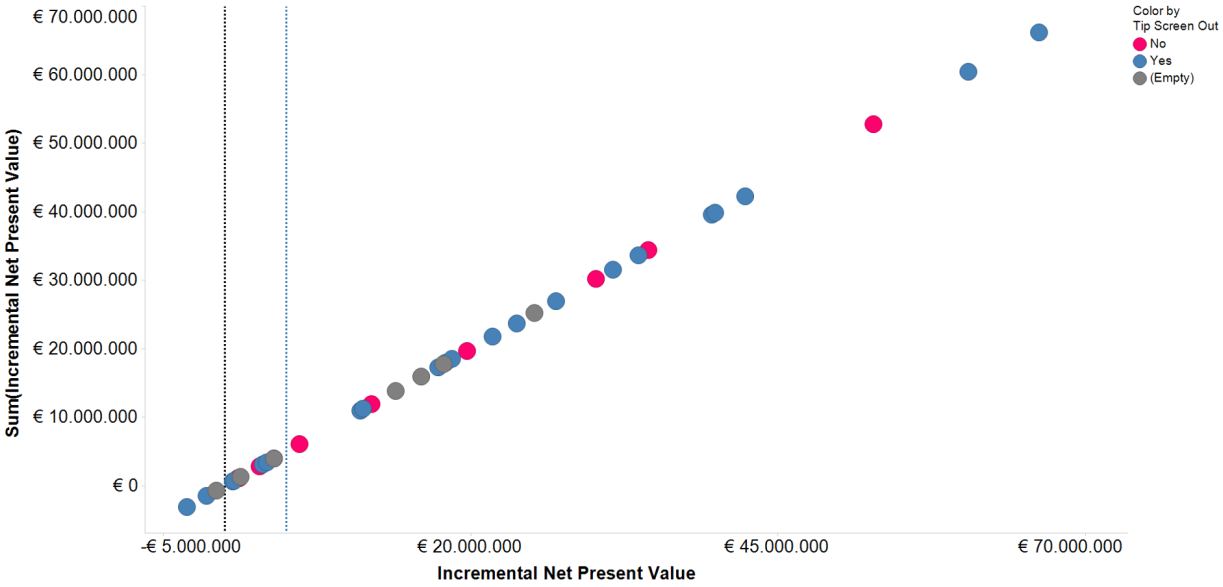


Figure C.14: The increment in net present value as function of the TSO. There is no trend observed since all datapoints are lying randomly on the line. For a considerably amount of wells the exact procedure of fracturing is not found in the treatment reports

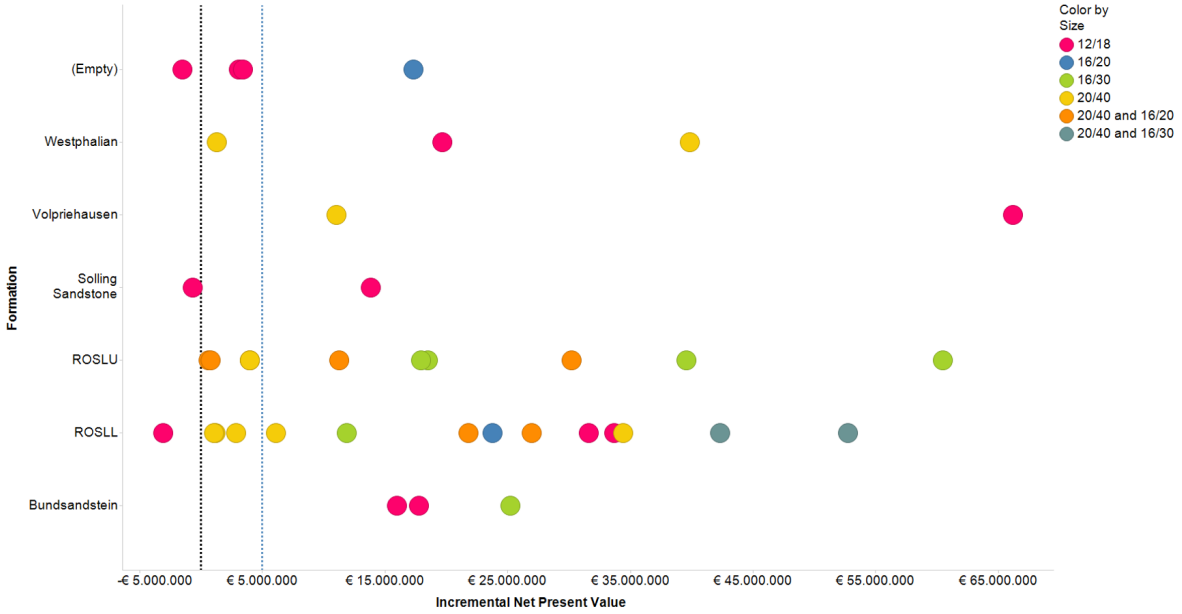


Figure C.15: The increment in net present value per formation. There is no trend observed since all datapoints are lying randomly on the line. The most wells that are fractured are in the upper and lower Rotliegend formation. For three wells the formation was not found.

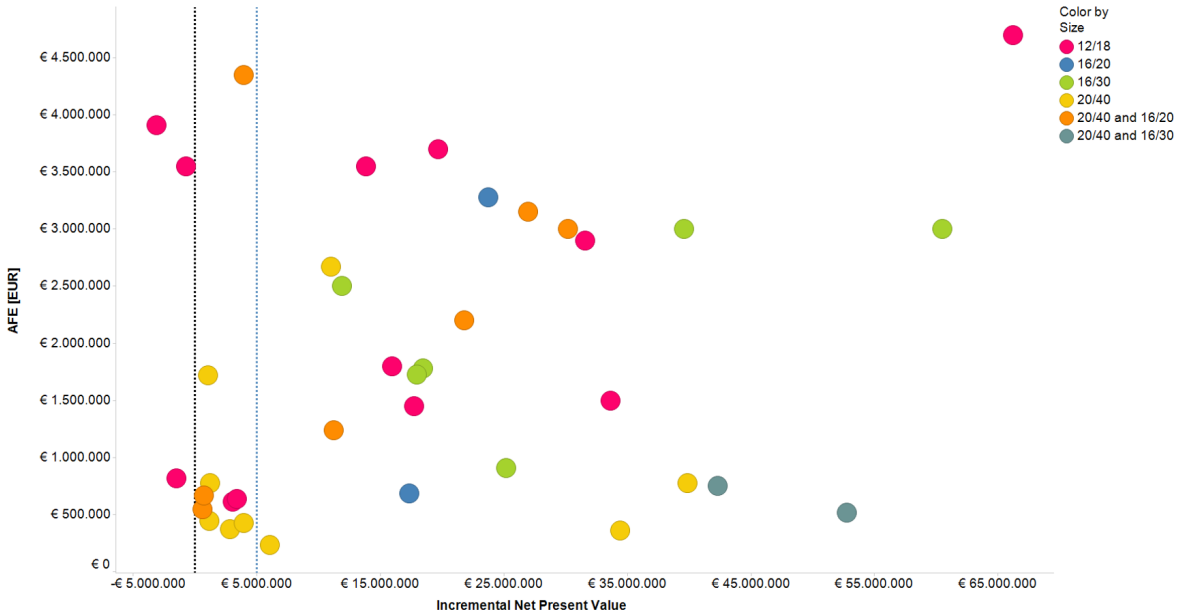


Figure C.16: The increment in net present value as function of authorization of expenditures (AFE), in this report the investment costs. A lot of datapoints which are lying in the lower NPV range are the cheaper treatments. However, the most negative NPV is also one of the most expensive treatments.

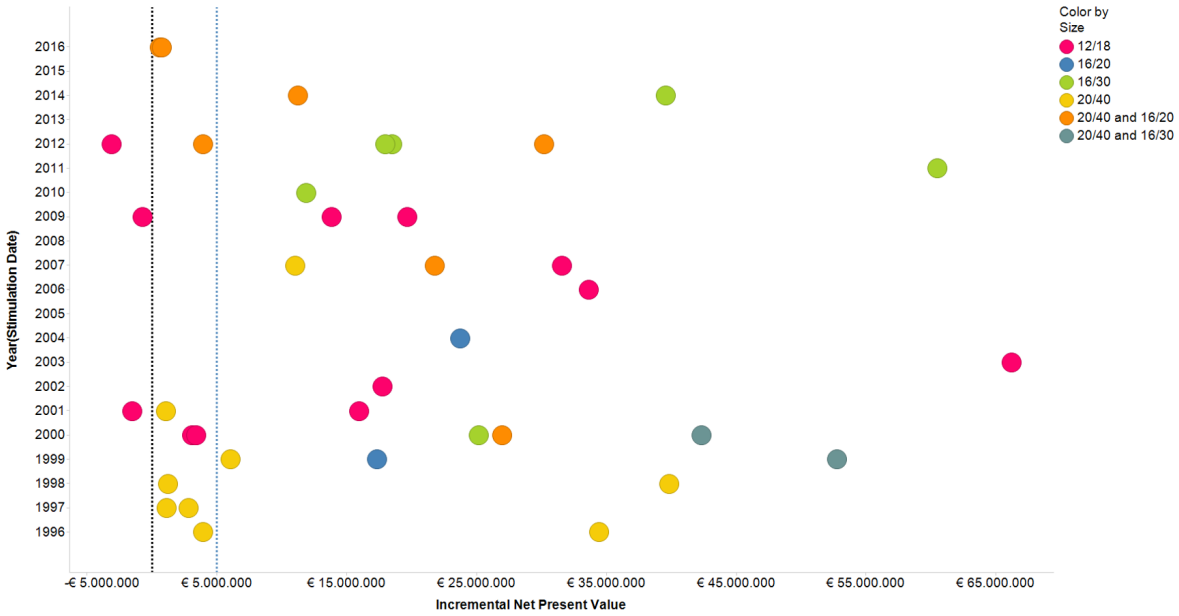


Figure C.17: The increment in net present value as function of the stimulation date. A lot of wells that are fractured before 2002 are in the negative NPV range.

# LIST OF FIGURES

# List of Tables

# BIBLIOGRAPHY


[1] E. B. Nederland, *Focus on dutch oil gas 2015,* Project **1**, 16 (2015).

[2] K. Hopstaken, *Inventory and analysis on hydraulically fractured wells in the dutch on- and offshore,* EBN **1**, 1 (2013).

[3] D. Mader, *Hydraulic proppant fracturing and gravel packing,* Elsevier: Developments in petroleum science 26 **26**, 16 (1989).

[4] C. T. Montgomery and M. B. Smith, *Hydraulic fracturing, history of an enduring technology,* JPT , 26 (December 2010).

[5] B. Brady, J. Elbel, M.Mack, H. Morales, K. Nolte, and B. Poe, *Cracking rock: Progress in fracture treatment design,* Oilfield Review **4**, 4 (1992).

[6] K. Armstrong, *Advanced fracturing fluids improve well economics,* Oilfield Review **7**, 4 (10/01/1995).

[7] G. E. King, *Hydraulic fracturing 101, what every representative, environmentalist, regulator, reporter, investor, university researcher, neighbor, and engineer should know about estimating frac risk and improving frac performance in unconventional gas and oil wells,* Society of Petroleum Engineers **20**, 2 (2012).

[8] S. op de Mijnen, *Resultaten inventarisatie fracking,* Report **1**, 1 (Februari, 2016).

[9] I. M. Inc., *Manual ihs harmony,* IHS Harmony Help **1**, 1 (2016).

[10] C. T. Montgomery and M. B. Smith, *Hydraulic fracturing,* CRC Press; Taylor and Francis Group **26**, 185 (2015).

[11] G. E. King, *Fracturing basics,* GEKEngineering.com **1**, 1 (2009).

[12] Y. Fan and F. Llave, *Tip screenout fracturing of gas wells,* SPE 35636 **1**, 463 (1996).

[13] J. W. Crafton and D. Gunderson, *Stimulation flowback management: Keeping a good completion good,* SPE 110851 **1**, 1 (2007).

[14] C. Montgomery, *Fracturing fluids,* Intech **1**, 4 (2013).

[15] Rigzone, *How does well acidizing work to stimulate production?* MPG Petroleum (2015).

[16] J. D. Arthur, *Evaluating implications of hydraulic fracturing in shale gas reservoirs,* SPE 121038 **1**, 1 (2009).

[17] K. P. Green and T. Jackson, *Managing the risks of hydraulic fracturing: An update,* Fraser Research Bulletin **1**, 1 (2015).

[18] E. P. Agency, *Assessment of the potential impacts of hydraulic fracturing for oil and gas on drinking water resources: Executive summary,* Environmental Protection Agency **1**, 1 (2015).

[19] A. V. Jackson, B. Robert, J. W. Carey, R. J. Davies, T. H. Darrah, F. O'Sullivan, and G. Petron, *The environmental costs and benefits of fracking,* Annual Review of Environment and Resources **39**, 1 (2014).

[20] R. Davies, G. Foulger, A. Bindley, and P. Styles, *Induced seismicity and hydraulic fracturing for the recovery of hydrocarbons,* Marine and Petroleum Geology **45**, 175 (2013).

[21] C. C. of Academics, *Environmental impact of shale gas extraction in canada: the expert panel on harnessing science and technology to understand the environmental impact of gas extraction,* Canadian Council of Academics **1**, 175 (2014).

[22] C. Whitson, *Cyclic shut-in eliminates liquid-loading in gas wells,* SPE 153073 **1**, 1 (2012).

[23] R. Turner, M. Hubbard, and A. Dukler, *Analysis and prediction of minimum flow rate for the continuous removal of liquids from gas wells,* J. Petroleum Technology **1**, 1475 (November 1969).

[24] C. et al., *A new look at predicting gas-well load-up,* J. Petroleum Technology **1**, 329 (March 1991).

[25] B. Okhuijsen, *Wellhead compression,* Presentation about multi well compression **1**, 3 (2014).

[26] J. Arps, *Estimation of primary oil reserves,* SPE 627-G **207**, 182 (1956).

[27] L. Matter and D. Anderson, *Dynamic material balance,* Petroleum Society **113**, 1 (2005).

[28] A. C. Gringarten and H. J. Ramey, *The use of source and green's functions in solving unsteady flow problems in reservoirs,* Society of Petroleum Engineers Journal **13**, 16 (1973).

[29] myElexys.be, *Ttf spotprice,* Website: https://my.elexys.be/MarketInformation/SpotTtf.aspx (2016).

[30] C. Santacruz, R. Esquivel, J. Smith, R. Walker, S. Bayer, T. Soto, M. Wunderle, A. Bansal, and R. Goudge, *Integration of rta based reservoir surveillance and analytical flow simulation to forecast production in the haynesville shale,* SPE-178560-MS/URTec:2153918 **1**, 1 (2015).

[31] H. Joo and S. Ki, *Rate transient analysis in hydraulic fractured tight gas reservoir,* SPE-176489-MS **1**, 1 (2015).

[32] S. Maxwell, *Beyond the srv: the epv provides a more accurate determination of reservoir drainage in shale reservoirs,* EP **1**, 1 (2013).

[33] P. Wie, C. Ehlig-Economides, D. Juan, H. Ying, and B. Song, *Intelligent rate transient analysis for forecasting behavior of shale gas wells,* SPE-1921855 **1**, 1 (2014).

[34] A. Duong, *Rate-decline analysis for fracture-dominated shale reservoirs,* SPE-137748 **1**, 1 (2011).

[35] E. Murminacho, H. Sanchez, M. Lopez, R. Rachid, J. Maniere, and A. Milne, *Increasing production and reserves in a mature field with hydraulic fracturing by combining fracture pressure analysis, pressure transient analysis and rate transient analysis,* SPE-177027-MS **1**, 1 (2015).

[36] C. Clarkson and P. Pedersen, *Tight oil production analysis: Adaptation of existing rate-transient analysis techniques,* CSUG/SPE-137352 **1**, 1 (2010).

[37] T. R. A. of Engineering, *Shale gas extraction in the uk: a review of hydraulic fracturing,* The Royal Society **1**, 9 (2012).